IDENTIFICATION OF WNT SIGNALING TARGETS IN NEMATODES

IDENTIFICATION OF PRY-1/AXIN MEDIATED WNT SIGNALING TARGETS IN *C. ELEGANS* AND *C. BRIGGSAE*

By

Jessica Knox, H.B.Sc.

A Thesis

Submitted to the School of Graduate Studies

In Partial Fulfillment of the Requirements

for the Degree

Master of Science

McMaster University

McMaster University MASTER OF SCIENCE (2014) Hamilton, Ontario (Biology)

TITLE: Identification of *pry-1/Axin* mediated Wnt signaling targets in *C. elegans* and *C. briggsae*

AUTHOR: Jessica Knox, H.B.Sc. (McMaster University)

SUPERVISOR: Professor Bhagwati P. Gupta

PAGES: ix, 96

Abstract

The Wnt signaling pathway plays a vital role in a multitude of cellular processes across a breadth of multicellular organisms, from simple nematode roundworms such as the *Caenorhabditis* species to humans. Through the study of this evolutionarily conserved signal transduction pathway in a simple model organism, a greater understanding of the regulation and function of the Wnt pathway can be gained. Emerging research is highlighting the promiscuous nature of Wnt signaling within the network of signaling pathways involved in *C. elegans* development and aging processes. However, impeding the study of the diverse roles of Wnt signaling in the nematode is the fact that little is known about regulation of key Wnt pathway components in the nematode species, and only a handful of downstream Wnt pathway target genes have been identified. We have used parallel genetic and genomic approaches to elucidate transcriptional targets of the Wnt pathway in *C. elegans* and the related species *C. briggsae.* This analysis has uncovered an array of putative Wnt pathway gene targets including *pry-1/Axin*, a key regulatory component of the pathway. Furthermore, our genome-wide search for Wnt targets has revealed a novel interaction between the Wnt and Hedgehog signaling pathways that is conserved between these two nematode species.

Acknowledgements

First and foremost I would like to thank Dr. Bhagwati Gupta for giving me the opportunity to learn and grow under his supervision in the lab. I truly appreciate your guidance and support throughout this sometimes arduous process. I would also like to thank my committee members, Dr. Roger Jacobs for all of his support over the years, and Dr. Rosa Da Silva for her extremely helpful comments during the thesis-writing process.

I am so appreciative of my colleagues in the Gupta lab, both past and present, for taking this journey with me and preparing me for the outside world, I hope I am ready! Thank you all for your advice and assistance (and the many, many coffee breaks) throughout the years, it will not be forgotten.

Last but not least, I would like to thank my family and friends; both those within LSB, and those who I could come to when I needed to escape LSB, for supporting me and making my Graduate School experience a memorable one. I will be forever grateful to you all.

Table of Contents

List of Figures

List of Tables

List of Abbreviations

AC - Anchor cell
Cbr - Caenorhabditis briggsae
Cel - Caenorhabditis elegans
EMS - Ethyl methanesulfonate
GFP- Green fluorescent protein
Hh - Hedgehog
HMG - High mobility group
Indel - Insertion-deletion polymorphism
L1 to L4 - Larval stages
Muv - Multivulva
PCR - Polymerase chain reaction
Pn.p - Ventrolateral P cell epidermal progeny
qRT-PCR - Quantitative real time polymerase chain reaction
RNA-seq - RNA sequencing
RNAi - RNA interference
SNP - Single nucleotide polymorphism
TF - Transcription factor
Unc - Uncoordinated
UTR - Untranslated region
VPC - Vulval precursor cell
WBA - Wnt/ β-catenin asymmetry pathway
WT- Wild type

Chapter 1 – Introduction

1.1 *Caenorhabditis elegans* as a model organism for developmental studies

At its core, biological progress in its many eclectic disciplines requires the use of genetic model organisms for simplified study of diverse and complex fundamental processes. *Caenorhabditis elegans* is a hermaphroditic nematode species that was introduced by Sydney Brenner as a simple model organism for genetic and developmental studies (Brenner, 1974). Since the establishment of *C. elegans* as a genetic model, it has become a cornerstone of invertebrate model research, contributing to advances in diverse fields of study such as cell death, developmental signaling, microRNAs and aging.

C. elegans offers many technical advantages as a model that make it amenable to laboratory studies. *C. elegans* is small, simple and economical to grow and maintain in large-scale populations on an *E. coli* food source. Other features of *C. elegans* that offer convenience in the lab include its high fecundity, producing upwards of 300 progeny per mother, and short lifecycle. In the *C. elegans* lifecycle, a self fertilized egg is laid, hatches, and proceeds through the larval stages (L1-L4) before becoming an egg-laying adult, all within ~3 days. *C. elegans* also has the ability to survive in conditions of starvation or overcrowding by entering a life stage known as dauer prior to entering the larval L3 stage. The worms can survive in the dauer stage for months and return to a normal life cycle when the conditions allow (Brenner, 1974). Additionally, *C. elegans* strains can

be frozen in liquid nitrogen for many years and remain viable when thawed, allowing a researcher to establish a working culture whenever necessary (Brenner, 1974).

Another unique feature of the *C. elegans* model is its transparent collagenous exoskeletal cuticle, which encloses the worm's tubular body containing the digestive, nervous, excretory and reproductive systems. This transparent cuticle allows for convenient visualization to the single cell level using differential interference contrast (DIC) microscopy. This ease of visualization allows for manipulation via single cell laser ablation, and gives us the ability to track the influence of genetic changes on individual cell fate, location, morphology and differentiation in an intact organism (Kimble and Hirsh, 1979; Sulston and White, 1980).

The *C. elegans* system has played host to a myriad of landmark scientific accomplishments. Not only was *C. elegans* the first multicellular organism to have its genome of more than 20,000 protein-coding genes completely sequenced (approximately 35% of which have known human homologs), it is the first and only animal to have its complete cell lineage mapped for each of the invariant somatic cells (959 in the adult hermaphrodite, and 1031 cells of the male) (Kimble and Hirsh, 1979; Sulston and Horvitz, 1977; Sulston et al., 1983; *C.e.*S. Consortium, 1998). Finally, a key contributor to its success as a model system, the simple nematode species *C. elegans* shares many developmentally

conserved pathways and processes with higher organisms including humans, allowing for the study of complex processes and gene regulatory networks in this simple system. These features, along with new genetic and molecular tools that are constantly being developed in this bourgeoning model system, have laid the groundwork for the use of this organism as a paradigm for the study of the genetic control of conserved developmental processes, and how the perturbation of these processes leads to human disease.

1.2 *Caenorhabditis briggsae* as a model for comparative developmental studies

Caenorhabditis briggsae is the closest known relative of *C. elegans.* Though they diverged from a common ancestor an estimated 30 million years ago, *C. briggsae* shares nearly identical developmental and behavioural traits with *C. elegans,* including those that make it a preferred laboratory model, and is thus used extensively for comparative evolutionary studies between the two species (Cutter, 2008; Stein et al., 2003). Comparative studies of these two nematode species can illuminate evolutionary similarities and differences in signaling and regulation of genes and developmental processes, which can in turn elucidate how conserved pathways are regulated in higher organisms.

While many cellular and developmental processes appear to be conserved between these two species, there are several well described functional divergences between *C. elegans* and *C. briggsae,* which illuminate the potential

of the comparative approach when studying these related species. These differences include gene expression during excretory duct cell development, genes involved in sex determination, male tail development and development of the vulva (Gupta et al., 2007). Vulval morphogenesis in particular is a well-established model for comparative developmental studies between *C. elegans* and *C. briggsae*. Though vulva formation is morphologically identical between these two species, there are key differences in the underlying regulation of the genes controlling this process (Felix, 2007; Sharanya et al., 2012). Comparative analysis of the genes and regulators of vulval development and other developmental processes in these nematode species can elucidate mechanisms of genetic redundancy and how changes in regulation can affect survival and health of the organism as a whole.

To facilitate the study of *C. briggsae* in both a comparative and individual context, many genetic and molecular tools are being developed. For instance, the genome sequence has been completed for the *C. briggsae* tropical reference strain AF16, as well as identification and sequencing of numerous polymorphisms with the *C. briggsae* temperate mapping isolate HK104 (Koboldt et al., 2010). This has allowed for development of a SNP-based oligonucleotide microarray for rapid mapping of *C. briggsae* mutants (SNP-Chip mapping) and a polymorphism-based linkage map has been created to allow for PCR based cloning of mutations in *C. briggsae,* both of which have been used in this study. Additionally, tools for

mutant analysis and elucidation of genetic interactions also facilitate genetic studies and analysis of genetic networks. Along with adding strength to the comparative approach to the study of these nematodes, these powerful tools also lend strength to the individual study of *C. briggsae,* leading to the illumination of new pathway components and regulatory networks that have not previously been discovered in *C. elegans* due to genetic differences between these species (Hillier et al., 2007; Koboldt et al., 2010; Stein et al., 2003; Zhao et al., 2010).

1.3 Overview of the canonical Wnt signaling pathway

The Wnt signaling pathway is a key evolutionarily conserved signal transduction pathway involved in an array of cellular processes throughout development, such as polarity, migration, proliferation and differentiation, in all metazoans. The requirement for Wnt signaling continues after development is complete, as Wnt signaling is known to be essential for stem cell maintenance and tissue regeneration in vertebrates. Aberrant Wnt signaling activity, particularly due to activating Wnt pathway mutations, underlie a range of human pathologies, most notably cancers in tissues dependent on Wnt for self-renewal or repair such as the colon (Clevers and Nusse, 2012).

As described in Figure 1, canonical Wnt signaling acts through the effector β-catenin, a transcription factor that is stabilized in the cytoplasm upon activation of the Wnt pathway. Wnt signaling is initiated by the presence of the ligand, a member of the Wnt family of secreted lipid-modified glycoproteins, binding to the

heterodimeric receptor complex made up of the seven-transmembrane protein Frizzled (Fz) and a lipoprotein receptor family co-receptor protein (LRP5/6/Arrow). This activates binding of the tumor suppressor protein Axin to the cytoplasmic tail of LRP5/6, regulated by phosphorylation of the LRP5/6 tail by the serine-threonine kinases glycogen synthase kinase (GSK3β) and casein kinase 1 (CK1), and facilitated by binding of the Dishevelled (Dsh) protein to the cytoplasmic portion of Fz. Axin is a member of the destruction complex, which regulates Wnt pathway output by controlling the stability of β-catenin, targeting it for degradation in the absence of Wnt pathway activity. The binding of Axin to the receptor, effectively impairs the destruction complex function, and allows for intracellular β-catenin to accumulate. When high β-catenin levels have accumulated in the cytoplasm, β-catenin translocates into the nucleus where it interacts with TCF/LEF family transcription factors bound to conserved consensus binding sites on Wnt pathway target gene regulatory sequences, to form a bipartite transcriptional activator. Transcriptional co-activators and histone modifiers are recruited, thus modulating the transcription of the diverse target genes of the Wnt pathway, ranging from cell cycle regulators and developmental control genes to transcription factors and components of the Wnt pathway itself (Figure 1, reviewed in Clevers and Nusse, 2012). A complete list of known targets can be found at the Wnt Homepage: http://www.stanford.edu/group/nusselab/cgi-bin/wnt/.

In the absence of the Wnt ligand, β-catenin is isolated in the cytoplasm and targeted for degradation via phosphorylation by the destruction complex, made up of the tumor suppressor scaffolding proteins Axin and Adenomatous Polyposis Coli (APC), as well as the constitutively active GSK3β and CK1α kinases. β-catenin then undergoes subsequent ubiquitination and rapid degradation by the proteasome. In the absence of nuclear β-catenin, TCF/LEF factors associate with co-repressor factors such as Groucho, which interacts with histone deacetylases to regulate chromatin structure, and bind to DNA at Wnt-responsive genes. This represses Wnt target gene transcription (Figure 1, reviewed in Clevers and Nusse, 2012; Eisenmann, 2005).

Recent studies on endogenous Wnt signaling in *C. elegans,* as well as primary intestinal epithelium and colorectal cancer cell lines carrying activated Wnt pathway mutations, have provided new insight into this key regulatory step of the Wnt pathway (Li et al., 2012). Li et al. (2012) have found that in the absence of the Wnt ligand, β-catenin is not only phosphorylated, but is also ubiquitinated by the F-box protein β-TrCP, part of an E3 ubiquitin ligase complex, and targeted for rapid destruction by the proteosome all within the intact destruction complex. It has been suggested that this ubiquitination is mediated by APC. The complex components are then recycled for further β-catenin binding. Additionally, they have found, counter to the classic model of canonical Wnt signaling, neither a disassembly of the destruction complex nor an inhibition of phosphorylation of

Axin-bound β-catenin occurs upon activation of Wnt signaling. Wnt signaling activation induces the association of an intact destruction complex, complete with phosphorylated β-catenin, with the LRP co-receptor. This binding of the destruction complex to LRP blocks ubiquitination of β-catenin by β-TrCP, which dissociates from the complex, possibly mediated by an altered interaction with APC. This leads to destruction complex saturation by bound phosphorylated β-catenin. Thus, newly synthesized cytosolic β-catenin is free to accumulate and be ferried into the nucleus where it will interact with nuclear DNA-bound TCF/LEF transcription factors to activate transcription of Wnt target genes, shaping Wnt pathway regulated cellular processes (Figure 1, Clevers and Nusse, 2012).

1.3.1 Wnt signaling in *C. elegans*

C. elegans provides a viable model for studying the canonical Wnt signaling pathway as homologs for the core Wnt pathway components are contained within its genome (Table 1, modified from Sawa and Korswagen, 2013). Like *Drosophila melanogaster* and vertebrates, worms have multiple Wnt ligand encoding genes (*lin-44*, *egl-20, mom-2, cwn-1, cwn-2),* Wnt receptors (Frizzled family members *lin-17, mom-5, mig-1, cfz-2)* and Dishevelled proteins (*mig-5*, *dsh-1, dsh-2).* The *C. elegans* genome also encodes for conserved Wnt ligand processing and secretion proteins such as the Porcupine homolog (*mom-1)* and Wntless homolog (*mig-14).* Genetic analysis of these Wnt ligands and receptors indicate a high degree of functional redundancy, with a combinatorial

activity of multiple Wnts and Wnt receptors required to accomplish the varied Wnt-regulated developmental processes in *C. elegans*. It has also been revealed that multiple tissues could act as sources of Wnt, including the gonad, muscles, and cells in the tail region (Gleason et al., 2006; Herman et al., 1995; Inoue et al., 2004; Sawa and Korswagen, 2013; Whangbo and Kenyon, 1999; Zinovyeva et al., 2008). Studies of of the Wnt genes using reporter assays and single molecule mRNA fluorescent in situ hybridization (smFISH), has revealed that they are expressed in partially overlapping domains along at anterior-posterior axis at the L1 stage. There is also evidence that the Wnt ligands form an anterioposterior gradient to pattern cell fates. This expression pattern suggests a conserved mechanism for providing positional identify along the body axis (Coudreuse et al., 2006; Sawa and Korswagen, 2013). Homologs for CK1α (*kin-19*), GSK3β (*gsk-3*), APC (*apr-1),* β-TrCP (*lin-23)* and transcriptional co-repressors such as Groucho (*unc-37*) also exist in the *C. elegans* genome.

A key difference between the Wnt pathway in the nematode and that of vertebrates is the presence of multiple genes encoding divergent β-catenin proteins (*bar-1, sys-1, wrm-1* and *hmp-2)* with distinct functions. BAR-1 is the sole β-catenin thought to be regulating canonical Wnt pathway dependent developmental processes. WRM-1 and SYS-1 are involved in a divergent canonical Wnt pathway that controls asymmetric cell divisions along the anterior-posterior axis of the worm (termed the Wnt/ β-catenin asymmetry pathway or

WBA). The WBA pathway notably controls the asymmetric cell division of the EMS blastomere in the 4-cell embryo stage into the anterior MS (mesoderm precursor) and posterior E (endoderm precursor) blastomeres, as well as asymmetric cell divisions during the development of the somatic gonad. Additionally, the WBA pathway is required for proper stem-cell like asymmetric division of the epithelial seam cells during larval development. The Wnt/ β-catenin asymmetry pathway is considered divergent, though it involves many components of the canonical Wnt pathway, due to its distinctive regulation involving asymmetric localization of Wnt signaling components as opposed to β-catenin stabilization. The final *C. elegans* β-catenin, HMP-2, is predominantly involved in cell adhesion, and does not appear to act in Wnt signaling. Additional differences include the two Axin-like proteins that regulate canonical Wnt signaling in the nematode (*pry-1* and *axl-1),* and the presence of a single TCF/LEF gene (*pop-1*) in contrast to the four found in vertebrates. Interestingly, no homolog has been identified for the LRP-5/6/Arrow, which is considered an essential Wnt pathway component in vertebrates. However, since nematode Wnt pathway genes are substantially diverged from their mammalian counterparts it is possible a homolog has been overlooked to date (Eisenmann, 2005; Gleason and Eisenmann, 2010; Lin et al., 1995; Miskowski et al., 2001; Oosterveen et al., 2007; Sawa and Korswagen, 2013).

1.3.2 Role of Wnt signaling in nematode vulval development

The canonical Wnt pathway acts through β-catenin homolog BAR-1 to influence a variety of developmental processes in *C. elegans* and *C. briggsae.* Putative downstream targets of canonical Wnt signaling in *C. elegans* include three Hox genes, *mab-5* (*Antennapedia/Ultrabithorax/ abdominal-A (Antp/Ubx/Abd-A) family*), *lin-39* (*Deformed/Sex combs reduced (Dfd/Scr*) *family*) *and egl-5* (*Abdominal-B (Abd-B) family*), that are involved in cell fate specification in numerous tissues. These Hox genes control processes such as neuronal differentiation and migration of the Q neuroblast progeny, male hook formation, fate specification of the posterior hypodermal P12 cell, and Vulva Precursor Cell (VPC) fate specification (Figure 2, Eisenmann, 2005). It should be noted that while these Hox genes have been found to function downstream of the Wnt signal, none have been shown to contain essential POP-1 binding sites, or have been found to be directly bound by POP-1, and thus cannot be classified as direct Wnt pathway targets.

In particular, the *C. elegans* vulva has been extensively used to study Wnt signaling pathway function and regulation in nematodes. The patterning and formation of the hermaphrodite vulva is tightly regulated by three conserved signaling pathways, LET-60/Ras-MPK-1/MAPK, LIN-12/Notch, and Wnt-BAR-1/ β-catenin (Eisenmann, 2005; Greenwald, 2005; Sternberg, 2005). These pathways interact during vulval development to confer an invariant cell fate

pattern of 3°-3°-2°-1°- 2°-3° on the 6 multipotent Vulval Precursor Cells (VPCs), which will then divide and form the mature vulva. Wnt signaling pays a role in maintaining VPC competence, promoting 2° fate and controlling cell polarity via regulation of Hox gene *lin-39,* and mutations in Wnt pathway components result in defective cell proliferation and division during vulval development in both *C. elegans* and *C. briggsae*. (Figure 2). The robust patterning of the vulva serves as a paradigm for the study of signal transduction and the complex integration of conserved signaling pathways controlling organ formation in both *C. elegans* and the related species *C. briggsae* (Eisenmann et al., 1998; Gleason et al., 2002; Seetharaman et al., 2010; Sternberg, 2005).

1.4 The structure and function of *pry-1/Axin* in nematodes *C. elegans* and *C. briggsae.*

Axin is a member of the destruction complex that acts to regulate cellular levels of Wnt pathway effector β-catenin. Axin is a scaffolding protein that interacts with both β-catenin and the other destruction complex members, tumor suppressor protein APC and serine-threonine kinases CK1 and GSK3β. Axin is the rate-limiting factor in destruction complex function, as it is present at low cellular concentrations (Lee et al., 2003). There are two vertebrate Axin genes, Axin1 and Axin2, also known as Conductin or Axil. These Axins are functionally equivalent *in vivo*, and both act as negative regulators of Wnt signaling, however Axin1 is constitutively expressed, while Axin2 is a global transcriptional target of

Wnt signaling and acts in a negative feedback loop to regulate pathway activity (Chia and Costantini, 2005; Jho, 2002; Lustig, 2002; Yan, 2001). As a key Wnt pathway regulator, Wnt-activating Axin mutations in humans are known to cause predisposition to colon cancer and tooth agenesis, and loss-of-function Axin mutations have been found in both colorectal and hepatocellular carcinomas (Lammi et al., 2004; Liu et al., 2000; reviewed in Clevers and Nusse, 2012).

Initially, no Axin homologs were identified in the *C. elegans* genome sequence (Ruvkun and Hobert, 1998). However, a yeast two-hybrid screen for proteins interacting with the armadillo repeat region of BAR-1/β-catenin identified the PRY-1 protein. The PRY-1 protein shares limited amino acid sequence similarity to vertebrate and *Drosophila* Axin, and related protein Conductin, family members (18-21%). The bulk of the sequence identity lies within the conserved RGS domain, which interacts with APC, and the carboxy-terminal DIX domain, which promotes interaction with Dishevelled (Korswagen et al., 2002). While no GSK3β and β-catenin binding domains were identified in PRY-1 based on sequence similarity, *C. elegans* PRY-1 was shown to interact with BAR-1/β-catenin, GSK-3/ GSK3β and the APC related protein APR-1, acting as a negative regulator of canonical Wnt signaling in the nematode. PRY-1 can also functionally interact with the destruction complex components in vertebrates, as overexpression of PRY-1 is seen to rescue the Masterblind Axin mutation in Zebrafish, and inhibits Wnt signaling in mammalian cells (Korswagen et al.,

2002). Additionally, epistasis analysis revealed that *pry-1* functions downstream of *egl-20/Wnt* and *mig-5/Dsh,* and upstream of *bar-1/β-catenin, pop-1/Tcf* and Wnt pathway target gene *mab-5* (Korswagen et al., 2002). Thus, it was determined that *C. elegans pry-1* encodes a functional, though divergent, Axin homolog which regulates canonical Wnt signaling in the nematode. A second Axin-like protein, AXL-1, has also been discovered in *C. elegans,* which is another highly divergent but functional Axin homolog. Though they exhibit some redundant functions during development, these two Axin homologs are not functionally interchangeable, unlike vertebrate Axin and Conductin, indicating that the function of Axin may be divided between these Axin orthologs in negatively regulating canonical BAR-1/β-catenin Wnt signaling during *C. elegans* development (Oosterveen et al., 2007). As much less is known about AXL-1 compared to the well-characterized PRY-1 Axin homolog, this has not been the focus of the present study.

The *C. briggsae* Axin homolog was later identified in a forward genetic screen, functioning upstream of canonical Wnt pathway components *Cbr-bar-1 (*β-catenin*)* and *Cbr-pop-1 (tcf/lef),* as well as Wnt pathway Hox gene target *Cbr-lin-39* (Seetharaman et al., 2010). Gene and protein structure of *C. elegans* and *C. briggsae* PRY-1 were compared, and show 70% conservation in overall protein structure between the two species, with higher percentages in conserved N-terminal RGS and C-terminal DIX domains (83% and 84% similarity

respectively), as well as the GSK3β and β-catenin binding domain (72% similarity). This degree of conservation between *C. elegans* and *C. briggsae* is similar to that of the APC homolog APR-1 (77% identical), but lower than that of the GSK-3β homolog GSK-3 (95% identical) (Korswagen et al., 2002; Seetharaman et al., 2010). At the gene level, it was found that *Cbr-pry-1* features the absence of one exon, as well as increased size of two introns when compared to *C. elegans* (Figure 3, Seetharaman et al., 2010).

pry-1/Axin mutants in *C. elegans* are well characterized. The *mu38* allele is a nonsense mutation, a G to A transition resulting in a premature stop codon in the seventh exon. *nc1* is also a nonsense allele, a C to T transition resulting in a stop codon in the second exon (Figure 3, Korswagen et al., 2002; Maloof et al., 1999; Shioi et al., 2001). An EMS mutagenesis screen was more recently completed in *C. briggsae* to study the evolution of the mechanism of vulval development between nematode species. Mutants were identified that display ectopic vulval cell proliferation and formation of multiple pseudovulvae. 3 alleles of *Cbr-pry-1/Axin* were obtained from this screen, *sy5353, sy5411,* and *sy5270.* Two of these, *sy5353* and *sy5411,* introduce premature in-frame stop codons, suggesting they are hypomorphic alleles. The *sy5353* allele is a G to A transition that disrupts the fifth splicing junction, affecting the donor site in intron six. *sy5411* has a 2 base insertion (GC) in exon five. No mutation was detected in the exons or junction sites in the *sy5270* allele animals suggesting this mutation may be

located in a regulatory region (Seetharaman et al., 2010).

As Wnt signaling is involved in many aspects of nematode development, these *pry-1/Axin* mutants display an array of phenotypes due to the perturbed regulation of this signaling pathway. Most notably, *pry-1* mutants of both species exhibit ectopic VPC induction as a result of the constitutive activation of the Wnt pathway in these cells, as previously described. This results in the Multivulva phenotype (Muv), in which additional ventral protrusions or "pseudovulvae" are formed from VPCs in both *C. elegans* and *C. briggsae* (31% and 93% penetrance in *mu38* and *sy5353* respectively, Figure 2) (Gleason et al., 2002; Seetharaman et al., 2010). Interestingly, the relatively weak Muv phenotype observed in *C. elegans pry-1* mutants is intensified in *pry-1(mu38) axl-1(tm1095)* double mutants to a penetrance of 96%, while mutations in *axl-1(tm1095)* alone exhibit 100% wild type vulva induction, suggesting these Axin-like proteins are acting together to control Wnt pathway function in this developmental process (Oosterveen et al., 2007). Additionally, a unique vulva phenotype is described in *pry-1* mutants, in which P7.p remains uninduced in a subset of mutant animals (25% in *mu38,* 80% in *sy5353).* This results in both an over- and under-induced vulva phenotype in these mutants. A genetic analysis of this induction defect phenotype revealed that it is caused by altered regulation of the Notch receptor family member *lin-12,* and its transcriptional target *lip-1* (a MAP kinase phosphatase), revealing an interaction between these two conserved signaling pathways in vulva

development (Seetharaman et al., 2010). A subset of *Cbr-pry-1(sy5353)* animals exhibit another facet of the VPC specification phenotype, in which the nuclei of entire posterior set of VPCs (P7.p-P11.p) appear smaller in size, morphologically similar to P12.pa. This phenotype was also observed in P7.p to P12.p in *Cel-pry-1* (*mu38*) mutants with a decreasing prevalence in fate transformation towards the anterior side (Pénigault and Félix, 2011; Seetharaman et al., 2010).

In addition to the vulval induction defects, *pry-1* mutants exhibit several characteristic developmental phenotypes. For instance, alterations are seen in Q neuroblast progeny migration, and in the formation of the male tail (Eisenmann, 2005; Seetharaman et al., 2010). The canonical Wnt signaling pathway controls the expression of Hox gene *mab-5* in the Q neuroblast lineage. The Q cell migratory neuroblasts are born at similar positions on the right (QR) and left (QL) side of the animal. In wild type animals, the QL cell and its descendants express *mab-5* and migrate towards the posterior of the animal, while descendent of sister cell QR do not express *mab-5* and migrate into the anterior. In mutants that result in reduction of Wnt pathway activity and thus *mab-5* expression, both QR.d and QL.d migrate towards the anterior. In *pry-1* mutants the opposite occurs, *mab-5* is ectopically expressed and both QR and QL descendants migrate into the posterior in a *bar-1/β-catenin* dependent fashion (Eisenmann, 2005; Korswagen et al., 2002). Additionally, the male population of both *C. elegans* and *C. briggsae* *pry-1/Axin* mutants feature additional phenotypes in the male tail. Unregulated

mab-5 expression in the seam cells results in the generation of ectopic sensory rays from these cells. Other male tail morphologies include crumpled spicules and pseudovulvae-like structures (Maloof et al., 1999; Sawa and Korswagen, 2013; Seetharaman et al., 2010). Though the regulation of *pry-1/Axin* is not yet well understood in these nematode species, these mutant phenotypes underline the developmental importance of proper regulation of *pry-1/Axin,* and the Wnt signaling pathway as a whole.

1.5 The goal of this study

The Wnt signaling pathway plays a vital role in a multitude of cellular processes across a breadth of multicellular organisms, from simple nematode roundworms such as the *Caenorhabditis* species to humans. Through the study of this evolutionarily conserved signal transduction pathway in a simple model organism, a greater understanding of the regulation and function of the Wnt pathway can be gained and therapeutic targets for treatment of human Wnt signaling related diseases can be uncovered. Emerging research is highlighting the promiscuous nature of Wnt signaling within the network of signaling pathways involved in *C. elegans* development and aging processes. However, impeding the study of the diverse roles of canonical Wnt signaling in the nematode is the fact that little is known about regulation of key Wnt pathway components in the nematode species, and only a handful of downstream Wnt pathway target genes have been identified, none of which overlap with those identified in other species.

By using genetic and genomics techniques to elucidate the transcriptional gene targets of the Wnt pathway in *C. elegans* and the related species *C. briggsae,* and concurrently dissecting the regulation and expression of *pry-1/Axin*, a key regulatory component of the pathway, we hope to gain a further understanding of the dynamics of Wnt pathway function, regulation and evolution in the nematode.

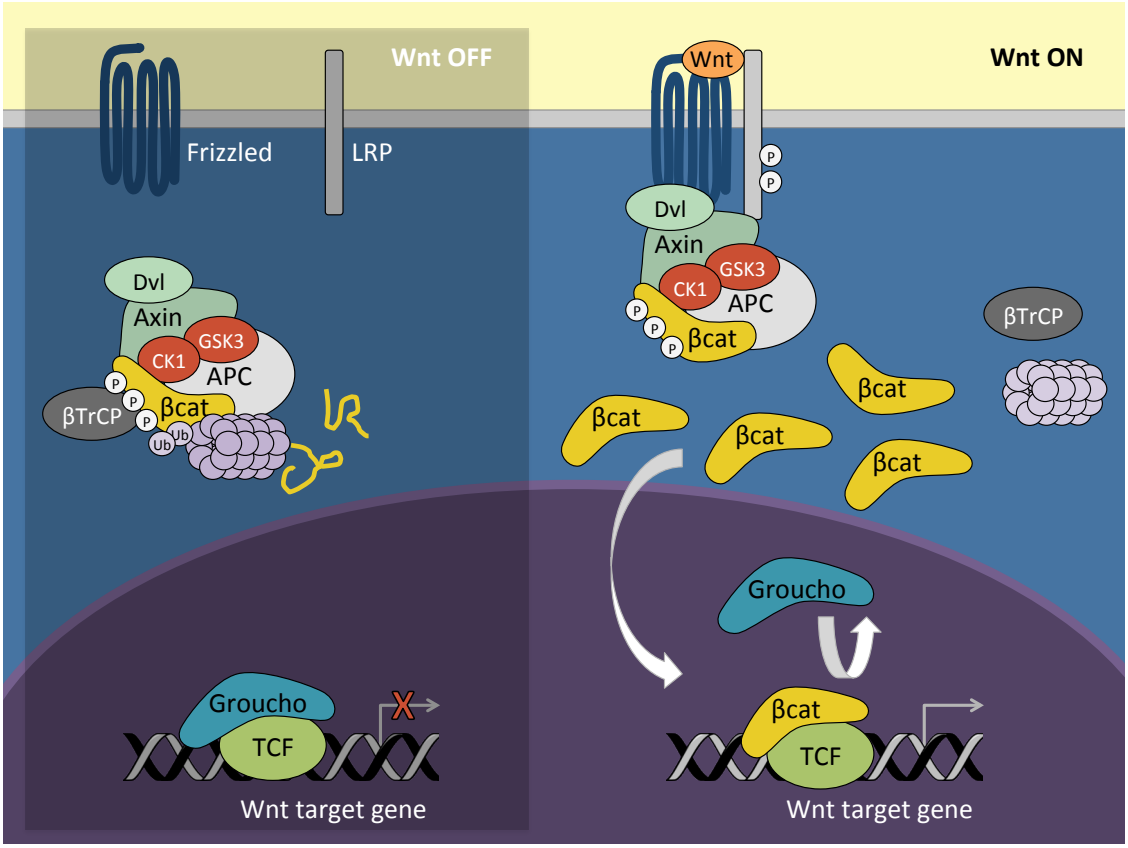

Figure 1. The current model of the Wnt signaling pathway. In the absence of the Wnt ligand, the destruction complex, made up of scaffolding proteins Axin and APC, along with CK1 and GSK3β kinases, binds β-catenin, where it is phosphorylated, ubiquitinated by β-TrCP and subsequently degraded by the proteasome, freeing the complex to bind additional β-catenin proteins. The TCF transcription factor is bound by co-repressors such as Groucho in the nucleus and represses Wnt target gene transcription. Upon Wnt ligand binding to the Frizzled receptor and LRP co-receptor, the destruction complex is bound to LRP, but is still able to bind and phosphorylate β-catenin. However, upon destruction complex binding to the LRP co-receptor, β-TrCP disassociates from the complex and thus ubiquitination and subsequent degradation of β-catenin is blocked. As a result, newly synthesized β-catenin builds up in the cytoplasm, and translocates to the nucleus. β-catenin replaces the Groucho co-repressor from TCF, forming a bipartite transcriptional activator complex which results in Wnt target gene transcription.

Table 1. *C. elegans* Wnt pathway components.

Component Name	Functional Classification	Number of Homologs			*C. elegans* Components
		Vertebrates	*Drosophila*	*C. elegans*	
Wnt	Wnt Ligands	19	7	5	LIN-44, EGL-20, MOM-2, CWN-1, CWN-2
Frizzled	Wnt Receptors	10	4	4	LIN-17, MOM-5, MIG-1, CFZ-2
LRP5/6		2	1	None	
Dishevelled	Wnt Signaling Effector Proteins	4	1	3	MIG-5, DSH-1, DSH-2
APC	Destruction Complex	2	2	1	APR-1
Axin		2	1	2	PRY-1, AXL-1
GSK-3β		2	1	1	GSK-3
CK1 α		1	1	1	KIN-19
β-Catenin	Transcriptional Activator	1	1	4	BAR-1, WRM-1, HMP-2, SYS-1
TCF/LEF	DNA binding Transcription Factors	4	1	1	POP-1

Names and functional classification of the core conserved Wnt pathway component homologs in *C. elegans* (Sawa and Korswagen, 2013).

A

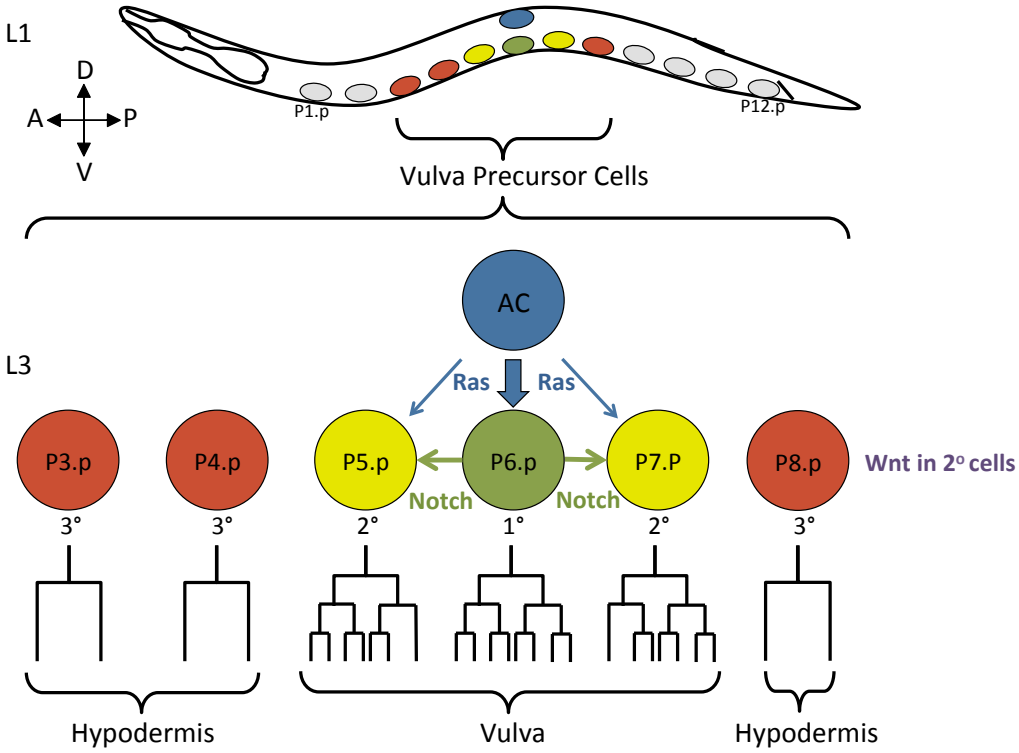
L1
D
A
P
V
P1.p
P12.p
Vulva Precursor Cells
AC
L3
Ras
Ras
P3.p
P4.p
P5.p
P6.p
P7.P
P8.p
Wnt in 2° cells
Notch
Notch
3°
3°
2°
1°
2°
3°
Hypodermis
Vulva
Hypodermis

B

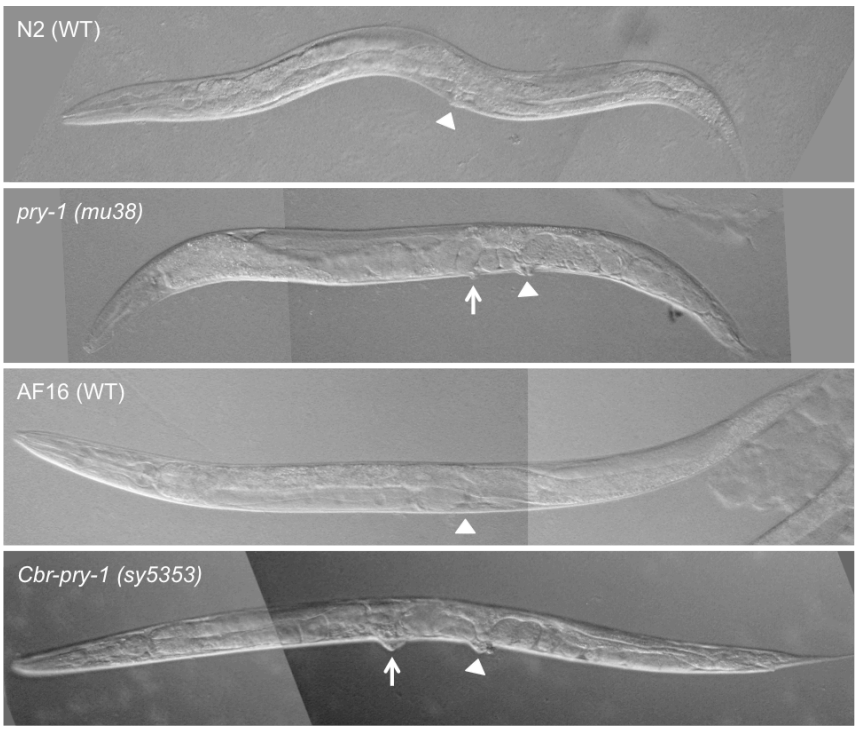
N2 (WT)
pry-1 (mu38)
AF16 (WT)
Cbr-pry-1 (sy5353)

Figure 2. The nematode Wnt signaling pathway is required for proper vulva morphogenesis. During vulva development, the Wnt pathway interacts with the Ras and Notch pathways to confer an invariant cell fate pattern of 3°-3°-2°-1°- 2°-3° on the 6 VPCs, P3.p to P8.p, which will then proceed to divide and form the mature vulva. Briefly, a LIN-3 inductive signal emanates from the anchor cell (AC) to activate the Ras/MPK pathway in P6.p promoting the acquisition of the 1° fate. Both LIN-3 mediated inductive signaling and LIN-12/Notch mediated lateral signaling confer 2° fate on P5.p and P7.p. Wnt signaling is involved in maintaining VPC competence, promoting 2° fate and P7.p polarity (A). When a key negative regulator of the Wnt pathway, *pry-1/Axin,* is mutated, Wnt signaling is constitutively activated. This results in a Multivulva phenotype in which the worm exhibits the formation of multiple pseudovulvae due to ectopic VPC induction. Arrowheads indicate the functional vulva and arrows indicate ectopic pseudo-vulvae protrusions in *Cel-pry-1(mu38)* and *Cbr-pry-1(sy5353)* adult animals (B).

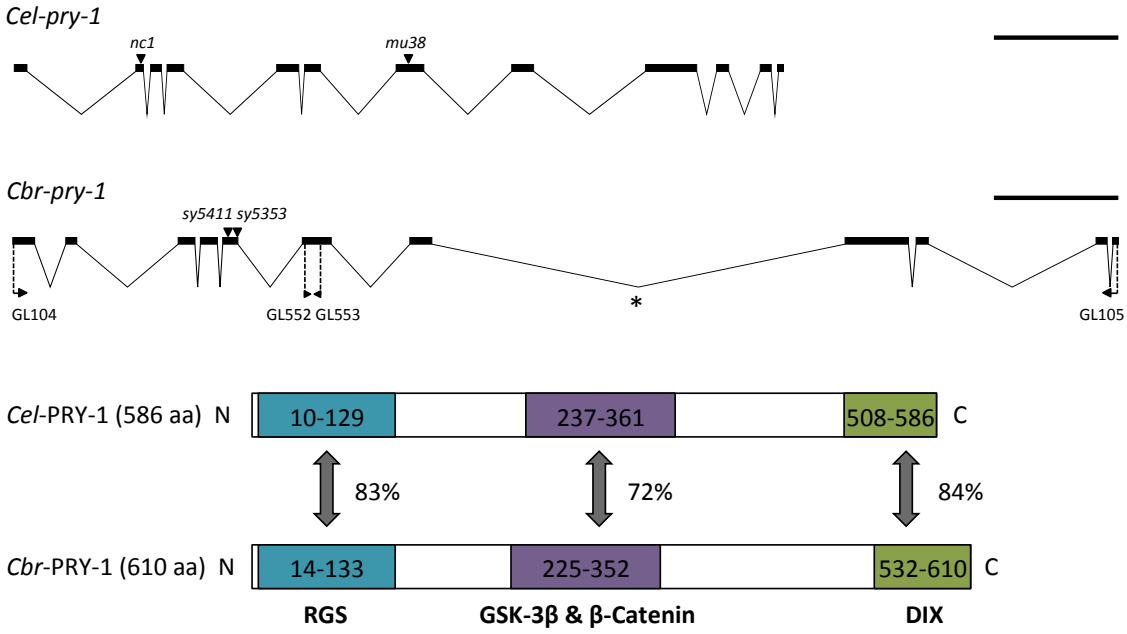

Figure 3. Comparison of *pry-1* gene and protein structure in *C elegans* and *C. briggsae*. Key structural differences include one fewer exon and two longer introns in the *C. briggsae pry-1* gene, and a 4% larger protein in *C. briggsae.* The exact length of *Cbr-pry-1* intron 7 (*) is unknown. The known mutation sites present in each mutant allele used in this study, as well as the location of sequencing primers used in this study are indicated. Scale bar indicates 1kb.

Chapter 2 - Materials and Methods

2.1 Strains and general methods

General methods for nematode culturing, maintenance and genetic manipulation were followed as previously described (Brenner, 1974). All experiments were carried out at 22°C unless otherwise stated.

The nematode mutant and transgenic strains used in this study are listed below, with the affected chromosome indicated where applicable. The prefix *'Cbr'* denotes the *C. briggsae* ortholog of a *C. elegans* gene.

Mutant Strains

C. elegans: N2 (wild type), *axl-1(tm1095) I, pry-1 (mu38) I, pop-1(hu9) I, bar-1(ga80) X*

C. briggsae: AF16 (wild type), *Cbr-pry-1 (sy5353) I , Cbr-pry-1 (sy5270) I , Cbr-pry-1 (sy5411) I, Cbr-pry-1(sy5353) I; sup4B, Cbr-pry-1 (sy5353) I; sup51D, Cbr-pry-1(sy5353) I* (10x introgression into HK104 background).

Transgenic Strains

C. briggsae: *mfIs42* [*sid-2::GFP; myo-2::dSRed*], *Cbr-pry-1(sy5353) I; mfIs42* [*sid-2::GFP; myo-2::dSRed*], *Cbr-unc-119 III; bhEx84* [*unc-119(+) + pGLC49 (cbr-pry-1p::GFP), Cbr-unc-119 III; bhEx86* [*unc-119(+) + pGLC48 (cbr-pry-1p::GFP), bhEx117* [*mec-7::GFP + myo-2::GFP*] (*bhEx117* is a transgenic HK104 strain).

Transgenic animals carrying extrachromosomal arrays were previously generated by standard microinjection technique using *unc-119* as a transformation marker (Maduro and Pilgrim, 1995; Mello et al., 1991). 50ng/µl concentrations of plasmids containing *Cbr-pry-1* 5' UTR fragments were

subcloned into Fire lab vector pPD95.69 to create *pGLC48 (Cbr-pry-1-2.4kb::GFP)* and*pGLC49 (Cbr-pry-1-3.8kb::GFP).* These were microinjected to create the transgenic lines that were used in this study (DY228 and DY226 respectively). These GFP reporter constructs were then crossed into the *Cbr-pry-1(sy5353)* mutant background for comparative studies, as described in Section 2.2.

2.2 Genetic crosses

Cbr-pry-1 5' UTR GFP reporter strains in the *Cbr-pry-1(sy5353)* mutant background were generated using the following genetic cross. Males of the wild type strain expressing the extrachromosomal *cbr-pry-1p::GFP* reporter in the wild type background were selected and mated to *Cbr-pry-1(sy5353)* mutant hermaphrodites. Five hermaphrodite progeny expressing GFP in the F1 generation were cloned onto separate plates at the L4 stage and allowed to self fertilize. In the F2 generation, 20 GFP expressing hermaphrodites were cloned singly onto plates at the L4 stage and those exhibiting the Multivulva phenotype associated with the *Cbr-pry-1(sy5353)* mutation in adulthood were selected for expansion. The penetrance of the Multivulva phenotype was monitored over the next several generations to confirm the presence of the *Cbr-pry-1 (sy5353)* mutation in these lines.

P *Cbr-pry-1(sy5353)/Cbr-pry-1(sy5353)* x *Cbr-pry-1p::GFP* ♂

↓

F1 *Cbr-pry-1(sy5353)*/+; *Cbr-pry-1p::GFP*

↓

F2 +/+; *cbr-pry-1p::GFP* →25%
Cbr-pry-1(sy5353)/+; *cbr-pry-1p::GFP* →50%
Cbr-pry-1(sy5353)/Cbr-pry-1(sy5353); *Cbr-pry-1p::GFP* →25% (selected for Muv)

2.3 Microscopy

Worms were mounted on agar pads in a solution of M9 buffer and the anesthetic sodium azide to immobilize the animals for viewing under the microscope. Various developmental stages were observed under Nomarski optics using Zeiss Axioimager D1 and Nikon Eclipse 80i microscopes. For GFP reporter expressing strains, epifluorescence microscopy was utilized using a Zeiss Axioimager D1 microscope equipped with the GFP filter HQ485LP (Chroma Technology). Images were taken using a Nikon DXM1200F digital camera and the Nikon ACT-1 software, and were processed using NIH Image J software.

2.4 Molecular biology

All primers used for traditional PCR, qRT-PCR and sequencing are listed in Table 2. *Cbr-pry-1* cDNA (1.9kb) was amplified for sequencing using primer set GL104 and GL105. The molecular position of sequencing primers located on *Cbr-pry-1* is presented in Figure 3.

2.5 RNA extraction and cDNA synthesis

2.5.1 Bleach synchronization

For large-scale synchronization of nematode populations, 10-40 100mm petri plates containing gravid hermaphrodites were bleached to obtain synchronized worm populations for RNA extractions. An alkaline hypochlorite solution was prepared using 1N sodium hydroxide (NaOH) and sodium hypochloride (commercial bleach) in a ratio of 3:2. For 1 volume of worms washed off their plates using M9 buffer and centrifuged in 15mL falcon tubes, at least 2.5 volumes of the bleach solution was added. The worms were vigorously shaken by hand in the alkaline bleach solution for no more than 10 minutes at room temperature. When all carcasses disintegrated and only eggs were visible in the solution, the eggs were pelleted and the bleach solution pipetted off, then washed 3 consecutive times in M9 buffer (Portman, 2005). At this point the embryos in M9 were plated onto agar plates and the F1 generation was allowed to grow at 20°C to the stage of interest for analysis. If a very high degree of synchronization was desired, a second round of bleach synchronization was performed on these F1 worms in which, when they developed to become gravid hermaphrodites, they were allowed to lay eggs for only 6 hours before they were collected and bleached a second time as described to obtain a more highly synchronized F2 population of animals.

2.5.2 Sample collection and total RNA extraction

Worms were grown on 100mm agar plates to an appropriate developmental time point and were collected and thoroughly washed several times in M9 buffer to remove any contaminating OP50 bacteria and other debris. Between 20-100µl of pelleted worms were generally collected in eppendorf tubes for optimal RNA extraction. Worm pellets were then flash frozen in liquid N_2 and stored at -80°C for subsequent RNA extraction.

A TRIzol-based method was used for total RNA isolation from the frozen worm samples (Portman, 2005). 4x the volume of TRIzol (Invitrogen, cat. no. 15596-026) was added to the volume of the harvested worm pellet and vortexed vigorously until completely resuspended. The sample was flash frozen in liquid N_2 then thawed at 37°C and vortexed. This was repeated 2 additional times. This freeze-cracking procedure acts to achieve lysis of the worm, disrupting the cuticle to allow for rapid RNA solubilization. 2-3 more volumes of TRIzol to the amount of starting worms was added and the sample was vortexed at room temperature for 30 seconds. The mixture was left to stand at room temperature for 5 minutes to disrupt all RNA-protein complexes. 2x the volume of the original worm pellet of chloroform was then added to the sample, followed by vigorous shaking for 15 seconds by hand. The sample was then left to stand at room temperature for 3 minutes and centrifuged at 12kg for 15 minutes at 4°C. The upper aqueous layer containing the RNA was then transferred to a fresh tube and the volume was

estimated. An equal volume of isopropanol was added to the aqueous layer. This solution was mixed well by hand and incubated at room temperature for 10 minutes, then centrifuged at 4°C at 12kg for 10 minutes. The RNA will have formed a gel-like pellet from which the supernatant was pipetted off, washed in 500µl of 75% ethanol, and centrifuged at full speed for 5 minutes at 4°C. This step was then repeated with the pellet washed a second time in 75% ethanol. The supernatant was carefully removed and the pellet was air-dried until all traces of ethanol evaporated (3 to 5 minutes). Care was taken to not over-dry the pellet until it became clear or resuspension would become difficult. The pellet was then dissolved in nuclease free water preheated to 55°C, with up and down pipetting used to aid in solubilization.

RNA samples were treated with RNaseOUT Recombinant Ribonuclease Inhibitor (Invitrogen cat. no. 10777-019) and DNase (Thermo Scientific DNase I, RNase-free, #EN0521). Quantity of the RNA was determined with spectrophotometric analysis using a GE Healthcare Life Sciences Ultrospec 2100 pro UV Spectrophotometer, and RNA purity was examined via the $A_{260/280}$ nm and $A_{260/230}$ nm absorbance ratios. Additional quality assessment for RNA integrity was completed by visual inspection of RNA for discrete 18S and 28S risbosomal RNA bands using a 0.8% agarose gel stained with ethidium bromide.

2.5.3 cDNA synthesis

The mRNA fraction of isolated total RNA preps was reverse transcribed to create cDNA using the NEB Protoscript AMV first strand cDNA synthesis kit (#E6500S). The recommended NEB protocol was followed. Briefly, 1-2µg of total RNA and 2µl of 50µM anchored oligo(dT) primers ($d(T)_{23}VN$) were combined with nuclease-free H_2O to a final volume of 8µl in two sterile RNase-free microfuge tubes, one for the reaction and one negative control. RNA was denatured by incubation at 70°C for 5 minutes. 10µl of 1x AMV reaction mix, an optimized buffer containing dNTPs, was added to both tubes. 2µl of AMV enzyme mix, containing AMV reverse transcriptase and RNase inhibitor, was added to one reaction tube, and 2µl of nuclease-free H_2O was added to the negative control tube (NRT, no reverse transcriptase control). This 20µl cDNA synthesis reaction was incubated at 42°C for one hour. The enzyme was then inactivated at 80°C for 5 minutes. Each reaction was diluted to 50µl with nuclease-free H_2O and stored at -20°C.

For those downstream experiments requiring higher concentrations of cDNA, a SIGMA M-MLV Reverse Transcriptase enzyme and 10X M-MLV Reverse Transcriptase Buffer for cDNA synthesis were used (product code M 1302) which allow for inclusion of 1-5µg of total RNA per 20µl final reaction volume. The recommended SIGMA cDNA synthesis protocol was followed.

2.6 qRT-PCR

Quantitative real-time PCR (qRT-PCR) was used to quantify and compare changes in gene expression levels between Wnt pathway mutants, and for validation of transcriptomics results. Reference gene *pmp-3* was used as an internal control in both *C. elegans* and *C. briggsae* qRT-PCR experiments based on the stability of its expression between biological samples (Hoogewijs, 2008). Reference genes are used for normalization in gene expression data analysis to correct for differences in the amount of cDNA template between wild type and mutant reactions. All qRT-PCR experiments were performed using SIGMA LuminoCt SYBR Green qPCR ReadyMix using a Bio-Rad CFX96 Touch Real-Time PCR Detection System. Data were generated and fold changes in gene expression analyzed using the Bio-Rad CFX manager software. A minimum of 2 biological replicates and 3 to 5 technical replicates were analyzed for each experimental condition, and a graphical representation of one or more of these biological replicates which is illustrative of the observed trend was created using Microsoft Excel. Cycling parameters were optimized to an initial denaturation step at 95°C for 2 minutes, followed by 40-50 cycles of a 10 second 95°C denaturation step and a 30 second combined annealing and extension step at a temperature optimized for each gene of interest. A sample reaction mixture for a single gene was as follows:

1 µl cDNA
5 µl LuminoCt SYBR Green qPCR ReadyMix
0.5 µl Forward Primer (10 µM)
0.5 µl Reverse Primer (10 µM)
3 µl Nuclease Free H_2O
10 µl per well total reaction volume

2.6.1 qRT-PCR primer design and optimization

Primers for qRT-PCR experiments were designed to span an intron to differentiate between genomic DNA contamination and cDNA. The primers were designed to amplify 80-200bp amplicons, the sequences of which were entered into the Mfold oligo analyzer (accessible from http://mfold.rna.albany.edu/?q=mfold) to examine the predicted secondary structure to optimize amplification efficiency. Primer pairs were then optimized for annealing temperature, product specificity based on melt curve analysis, and identity of amplicon product by examining PCR products on an agarose gel to confirm the appropriate amplicon size was produced. Lastly, an eight point standard curve was created from a serial dilution for each primer pair examined at their optimal annealing temperature. The slope of the standard curve allows one to calculate the efficiency of the reaction under these conditions, or the rate at which the enzyme converts cDNA template to amplicons. An efficiency value between 90-110% was considered optimal.

2.7 RNAi

RNAi by feeding was performed on agar plates containing 0.6% Na_2HPO_4, 0.3% KH_2PO_4, 0.1% NH_4Cl, 0.5% Casamino Acids, 2% Agar, 1mM $CaCl_2$, 1mM $MgSO_4$, 0.0005% cholesterol, 0.2% β-lactose, and 50 μg/ml Carbenicillin. Plates were seeded with 150μl of overnight grown HT115 bacterial culture in LB and Carbenicillin media that produces dsRNA of the gene of interest. Worms were bleach synchronized and the resulting embryos were placed on a rotator for 24 hours where they were allowed to hatch in M9 solution resulting in arrest at the L1 stage. Synchronized L1s were then plated on plates containing RNAi bacteria or the L4440 empty vector control at the L1 stage and allowed to grow until the stage of interest when they were then collected for analysis. RNAi experiments were performed in triplicate and batches that produced consistent results were analyzed.

For RNAi experiments in *C. briggsae,* transgenic strains were used that carry a wild type copy of the *C. elegans sid-2* gene, as *C. briggsae* is resistant to environmental RNAi. The presence of *C. elegans* SID-2*,* an intestinal luminal transmembrane protein, confers sensitivity to environmental RNAi to a degree similar to that seen in wild type *C. elegans* N2 (Winston et al., 2007).

2.8 Genetic mapping

2.8.1 Insertion-deletion (indel) and snip-SNP-based mapping

C. briggsae pry-1 Multivulva phenotype suppressor mutations were isolated in an EMS mutant screen. These mutations were mapped to chromosomes by bulk segregant analysis (BSA) using insertion-deletion (indel) polymorphisms and snip-SNPs (Koboldt et al., 2010). The mapping cross scheme that was used can be seen in Figure 11. Briefly, hermaphrodites of the mutant strain in an AF16 background were crossed with males of an HK104 background. Cross progeny in the F1 generation were cloned and allowed to self fertilize, allowing recombination to occur. 10 phenotypically mutant F2 worms were selected containing the putative mutation and were processed for genomic DNA extraction (Koboldt et al., 2010). Genomic DNA was extracted by placing worms into 10µl solution of lysis buffer containing Proteinase K. The solution was frozen in -80°C for one hour, then incubated at 60°C for one hour followed by heat inactivation of Proteinase K at 95°C and diluted with 10µl of nuclease free water. This genomic DNA prep was frozen at –20°C and used as a template for PCR testing of the polymorphic markers to determine linkage of the mutation site to different polymorphic loci in order to map the chromosomal location of the mutation.

The polymorphic markers used in this study for mapping these unknown mutations included both medium indels and snip-SNPs. Over 30,000

polymorphisms between the *C briggsae* reference strain AF16 and the natural isolate HK104 have been identified and described by Koboldt et al. (2010). These included conventional SNPs, SNPs that alter a restriction enzyme recognition site (snip-SNPs) and indels ranging in size from small (7-49 bp), to medium (50-2000 bp) to large (>2 kb). Small and medium indels are most suitable as genetic markers. Medium indels are most useful for initial mapping of the mutation to a larger scale chromosomal level, as their resolution by agarose gel electrophoresis is relatively easy, while small indel analysis is more difficult but very useful to further refine chromosomal position of mutations within the chromosome.

2.8.2 SNP-Chip-based genetic mapping

SNP-Chip mapping uses an oligonucleotide microarray containing 9701 well spaced SNPs between AF16 and HK104 across each of the chromosomes to identify and precisely map *C. briggsae* mutants (Zhao et al., 2010). The mapping cross used is similar to that for polymorphism mapping described in 2.9.1 (Figure 11), however 100 F2 worms were picked and allowed to reproduce for several generations. These worms were washed with M9 buffer and genomic DNA was extracted using the QIAGEN Blood and Tissue DNeasy kit (cat. no. 69504). This DNA was hybridized to the SNP Chip and differences in the hybridization signals between oligos of the array from AF16 and HK104 were detected for each SNP across each chromosome. The intensity of the mapping signal and the signal arc allowed for the extrapolation of the approximate

chromosomal location of the mutation of interest based on the ratio of AF16-type versus HK104-type DNA at each polymorphism on the Chip.

Table 2. List of oligonucleotide primers used in this study.

Locus	Oligo Name	Sequence (5' to 3')	Use
Cbr-pry-1	GL104	ATGGAGAGTGGACCATCATCTCATCTC	Sequencing
	GL105	ATAGCGAATCTCGGCAGCAATTCTTC	
	GL552	AGAATCGGGATACGGCTACAG	Sequencing and qRT-PCR
	GL553	CCTCTCCTTCCATTTTCGGTC	
Cbr-pmp-3	GL765	TGGAATTGAGAGTCAAGGGTCGCGG	qRT-PCR
	GL766	CAAGGAAACTAGCTGTTCGGCTGGC	
pmp-3	GL747	CTTAGAGTCAAGGGTCGCAGTGGAG	qRT-PCR
	GL748	ACTGTATCGGCACCAAGGAAACTGG	
pry-1	GL741	CGCCAACACGAGGAGTTTGTGG	qRT-PCR
	GL742	TGTGATGAATGGTGGGCGGAGC	
ptr-16	GL853	GCAATGCTTCATCCCGATTACATCC	qRT-PCR
	GL854	GTGGTTTGACGATCCGTTCGGA	
ptr-19	GL855	CATCAACTACCCATCAATCTGCGTG	qRT-PCR
	GL856	GATCCGAGACGAGAAGCAGCTTGA	
ptr-20	GL857	CATTTGTGCCGACGATTTCTCAGG	qRT-PCR
	GL858	GTGTTGACATGAGAGACGAGGGCA	
grd-14	GL876	TTTTCGTCGCCATCTCGTCT	qRT-PCR
	GL877	GGCATGCCTCTGGCTCATA	
grd-15	GL878	GCAACGGGATGAGCAGATAGA	qRT-PCR
	GL879	GGGTTGCAACACATGAAGC	
grd-6	GL880	TATTGCCCAGCCAAATCCAAGAGTCGT	qRT-PCR
	GL881	GTTGTGGTCTGTACTGTTGTTGGA	
grl-1	GL882	ACTGCCACAAGATATCAGGCAT	qRT-PCR
	GL883	TTGTAGAGTCGGTTGCTGGG	
grl-16	GL884	GCTTTGAAGAACGAGAAGGACAACC	qRT-PCR
	GL885	GTTTCTCTTTCCGTACCAGTTGACG	
grl-21	GL886	ACGGACCAGGACCATACAGA	qRT-PCR
	GL887	TCACCTGATGTCATTCCCTTCT	
grl-4	GL888	GGAGAGGAACATGAACGGTGA	qRT-PCR
	GL889	CTTGGCAGTAGGTCTCGGTG	
grl-6	GL890	GAGACCATCTTGCCCGTGTA	qRT-PCR
	GL891	GCAACAATCGTTCTGAGCTGG	
grl-13	GL892	GGAAGAGGCAATGTCGTCCA	qRT-PCR
	GL893	AAATCTGGCCGTCCAACTCC	
Cbr-grl-16	GL932	AAACTGCGACGATCCAGAGC	qRT-PCR
	GL933	CTCCGAATTTGGCTGAAGCG	
Cbr-qua-1	GL934	CGAAATATGCGGAGAAGGCAAAG	qRT-PCR
	GL935	GGTCATTCGGCCGATCCTAA	
cb-m142 (Chr 1)	GL588	AAGGCCTTAAAAATGAAGATAAT	Indel Mapping PCR
	GL589	TGAAAATTGAAAAACCTAGAAAA	
cb-m26 (Chr 2)	GL594	CGTTGAACATTAATTTGAAGAGT	Indel Mapping PCR
	GL595	AGACCAGAAGACTGGAATGAG	
cb-m46 (Chr 3)	GL596	GAATCCATGTGATTTGAGAGAC	Indel Mapping PCR
	GL597	TGGCTCAGAGTTGAGAGACT	
cb-m172 (Chr 4)	GL600	ACATTCATTAACAAATGCAGACT	Indel Mapping PCR
	GL601	ATCAAAAGCCCCATATAAACTT	
cb-m103 (Chr 5)	GL604	AGGTGAGAGTTTTTGACTTTCTT	Indel Mapping PCR
	GL605	TTACATTGTTCAGTTGGAAACTT	
cb-m127 (Chr x)	GL610	TGTGAGTGTATTGATTTTTATTAGC	Indel Mapping PCR
	GL611	GATGACAGGTGAAGTGAGAGA	
Cb48850 (Chr 4)	GL676	CTTTGGAAATCTTCATTCTGAT	Snip-SNP Mapping PCR
	GL677	CATATCCTCAATCCATGACTTC	

Chapter 3 – *pry-1/Axin* expression and regulation in *C. elegans* and *C. briggsae*

The Wnt signaling pathway is known to play a vital role in an array of cellular processes across the breadth of multicellular organisms. We aimed to gain a new depth of understanding of the regulation and function of this conserved pathway in the simple nematode model. Through the comparative study of this evolutionarily conserved signal transduction pathway in nematodes *C. elegans* and *C. briggsae*, new insight can be gained which can be translated into a better understanding of Wnt signaling in higher organisms, even allowing for the elucidation of therapeutic targets for treatment of Wnt signaling related human diseases. To gain a deeper understanding of the dynamics of Wnt pathway function, regulation and evolution in the nematode, we have undergone an investigation as to the regulation and expression of the nematode Axin homolog *pry-1,* a key conserved negative regulator of the Wnt pathway, in both *C. elegans* and *C. briggsae.*

3.1 *pry-1/Axin* expression is responsive to Wnt signaling activity in *C. elegans* and *C. briggsae*

The Wnt signaling pathway is known to use feedback control as a mechanism of self-regulation, via controlling the expression of several of its own signaling components. In particular, the Axin ortholog Axin2 is known to be a transcriptional target of the Wnt pathway in vertebrate species such as mice and humans (Jho et al., 2002; Lustig et al., 2002; Yan et al., 2001). To investigate if

pry-1/Axin is similarly regulated by the Wnt signaling pathway in nematodes, we examined the transcriptional expression levels of *pry-1* in response to Wnt pathway activity in both species.

The *pry-1* expression level was first examined using qRT-PCR in mixed stage and L1 stage synchronized populations of wild type (*C. elegans* N2 and *C. briggsae* AF16) compared to *pry-1* mutants in both species (*C. elegans mu38* and *C. briggsae sy5353, sy5411, and sy5270)*. The results show increased *pry-1* transcript levels compared to wild type in both *C. elegans pry-1* (*mu38)* and each of the three *C. briggsae pry-1* mutant alleles, as depicted in Figures 4 and 5. This was our first indication that *pry-1* expression may be regulated by Wnt pathway activity in these nematode species. A dramatic increase in *pry-1* expression is present in the two *C. briggsae* alleles containing identified missense mutations, *sy5353* and *sy5411* (6.9 and 5.2 fold increase respectively). In *Cbr-pry-1 (sy5270)*, for which no mutation site has been identified in the exons or exon-intron junctions, a less dramatic fold increase in *pry-1* expression is observed (2.3 fold increase). It is likely that the mutation site in *sy5270* is contained within a non-coding regulatory region. It is a possibility that this mutation may lie within a POP-1/Tcf binding site, which could result in the observed impaired response (increase in *pry-1* expression) to the heightened Wnt signaling pathway activity conferred by the *pry-1* mutation.

A more thorough investigation of *pry-1* expression across a range of

developmental time points was completed for the *Cbr-pry-1* allele *sy5353.* Bleach synchronization was used to analyze populations of *sy5353* animals at embryo, L1 and L4 larval stages. A dramatic increase in *pry-1* transcript level was observed in *sy5353* mutants compared to wild type at all stages tested (4.9, 3.8, and 7.0 fold increase in expression respectively, Figure 6).

We have observed that *pry-1* expression increases, corresponding with an increase in Wnt pathway activity. To further investigate the possibility that *pry-1* expression is being regulated by a positive feedback mechanism controlled by Wnt pathway activity, we examined *pry-1* levels in the mutant background of positive regulators of the Wnt pathway, resulting in a reduction of canonical Wnt pathway activity. This analysis of *pry-1* expression was completed in both the *C. elegans* TCF/LEF transcription factor *pop-1* hypomorphic mutant background at L1 and L4 stages, as well as a *bar-1/β-catenin* null mutant background at the L1 larval stage. A reduction in *pry-1* transcript level is observed when these key positive regulators of Wnt pathway activity are knocked down compared to wild type (0.53 and 0.38 fold expression respectively at L1 stage, and 0.52 fold expression in *pop-1(hu9)* at L4 stage), further substantiating our hypothesis (Figure 4). Interestingly, when *pry-1* level in the mutant background of the second *C. elegans* Axin homolog, *axl-1* (619bp deletion allele *tm1095*), a negative regulator of Wnt signaling activity, was examined at the L1 stage, a slight reduction in *pry-1* transcript level was observed compared to wild type (0.57 fold

expression, Figure 4).

3.1.1 The *pry-1* UTR contains conserved TCF/LEF family transcription factor POP-1 binding sites.

We have established that *pry-1* expression levels are responsive to Wnt pathway activity in both *C. elegans* and *C. briggsae*. However, what is still unclear is if *pry-1* is a direct transcriptional target of the Wnt pathway, acting through its downstream transcriptional effector TF POP-1. We performed a search for transcription factor binding sites within the *pry-1* 3' (500bp), 5' (2.5kb) and intronic UTRs in both *C. briggsae* and *C. elegans* using the bioinformatics program MatInspector Genomatrix v.8.0.0 (http://www.genomatix.de). TCF/LEF proteins bind DNA in a sequence-specific manner via a high mobility group (HMG)-box DNA binding domain. The conserved TCF/LEF transcription factor POP-1 binding sites (YTTTGWW) identified by the software were mapped and aligned, as depicted in Figure 7 (Cartharius, 2005). The presence of these sites can be used as a starting point to dissect the regulatory regions of *pry-1* in an attempt to establish whether *pry-1* is a direct transcriptional target of the Wnt signaling pathway.

3.1.2 *pry-1* expression in response to *pop-1* RNAi in *C. elegans* and *C. briggsae*

The presence of POP-1 binding sites in the *pry-1* UTR alludes to a direct target relationship between *pry-1* expression and Wnt pathway activity. Thus, we wanted to investigate the consequences of knocking down *pop-1* function on *pry-*

1 expression in both *C. elegans* and *C. briggsae.* The presence of multiple POP-1 binding sites suggest that a reduction in *pop-1* levels should result in a corresponding reduction in *pry-1* expression compared to wild type. We were also interested in determining if introducing *pop-1* RNAi in the *pry-1* mutant background would reduce the *pry-1* levels to a wild type level of expression, as it has been seen that the reduction of *pop-1* expression either by RNAi (in *C. briggsae)* or the hypomorphic *pop-1* mutant allele *hu9* (in *C. elegans)* partially suppresses the ectopic VPC induction defect in the *pry-1* mutant background (Gleason et al., 2002; Seetharaman et al., 2010). We have previously described the moderate decrease in *pry-1* expression observed in the *C. elegans pop-1(hu9)* mutant background at L1 stage. This was repeated at the L4 stage and a similar fold change was observed (0.51 fold expression of *pry-1* in the *pop-1(hu9)* mutant relative to wild type, Figure 4). However, as this *pop-1* allele is a weak hypomorphic mutant, and no mutant alleles have been isolated for *pop-1* in *C. briggsae,* we performed feeding RNAi experiments for *Cel-pop-1* and *Cbr-pop-1,* in both the wild type and *pry-1* mutant background, and harvested these worms at the L4 stage (*C. elegans*) or the young adult stage (*C. briggsae*) for qRT-PCR analysis to examine *pry-1* expression levels.

Interestingly, we found that while *pop-1* RNAi resulted in a slight decrease in *pry-1* expression in wild type *C. elegans* compared to N2 worms exposed to only the vector control L4440 (0.75 fold expression), the opposite was true for *C.*

briggsae (Figure 8). In the presence of *Cbr-pop-1* RNAi, wild type *C. briggsae* animals exhibit a 3.1 fold increase in *pry-1* expression compared to those exposed to the vector control. However, in both species, exposure of the *pry-1* mutants to *pop-1* RNAi resulted in a reduction of *pry-1* expression levels compared to the *pry-1* mutants exposed to the empty vector control L4440. In *C. elegans,* the fold expression of *pry-1* relative to the vector control in the wild type background reduced from a 2.5 fold increase seen in the *pry-1(mu38)* vector control, to a 1.5 fold increase in the presence of *pop-1* RNAi in the *pry-1(mu38)* mutant background (Figure 8). In *C. briggsae,* the *pry-1* expression levels changed from a 7.7 fold increase in the *pry-1(sy5353)* mutant vector control to a 5.8 fold increase relative to the vector control in the wild type background (Figure 8). This partial restoration of wild type *pry-1* expression levels coincides with the previous findings that describe a partial rescue of the *pry-1* mutant vulva phenotype on exposure to *pop-1* RNAi or in the presence of the hypomorphic *pop-1(hu9)* mutant background (Gleason et al., 2002; Seetharaman et al., 2010).

3.2 Sequencing of *Cbr-pry-1* transcript in the *sy5353* allele

We have observed a dramatic increase in *pry-1* mRNA expression in *C. briggsae pry-1* mutants. It is known that *Cbr-pry-1(sy5353)* is a splicing donor site mutant that introduces two in-frame stop codons within 40 bases of the mutation site. The primer pair used in our qRT-PCR experiments examining *pry-1* expression in this mutant is located downstream of this mutation site. The

heightened *pry-1* expression seen in our results suggests the presence of a cryptic donor splice site bypassing these stop codons, as their presence would typically initiate rapid degradation of the transcript by the nonsense mediated mRNA decay (NMD) pathway, making them difficult to detect (Hodgkin, 2005). Thus, we sequenced the full-length *pry-1* cDNA in the *sy5353* mutant using sequencing primers GL104, GL105, GL552, and GL553 (primer locations are indicated in Figure 3) to reveal any splicing errors resulting from this mutation. The sequencing data revealed several splice variants. Surprisingly, predominantly featured is a *sy5353* mutant transcript including a 31 base portion of intron 5 that contains an in-frame stop codon. Exon 6 sequence resumes at the point of a putative cryptic donor splice site within intron 5 closely resembling the 5' splice site consensus sequence GURAGU, as seen in Figure 9 (Blumenthal and Steward et al., 1997).

3.3 *Cbr-pry-1::GFP* reporter expression

For additional confirmation of our qRT-PCR findings in *C. briggsae*, *pry-1::GFP* reporter strains were created in both the wild type and *sy5353* mutant backgrounds. These reporter constructs were previously generated using 2.4 and 3.8 kb 5' UTR fragments of *Cbr-pry-1* subcloned into the Fire lab GFP expression vector pPD95.69 (Seetharaman et al., 2010). In the wild type background, expression of these reporters is visible throughout development in an array of cell types, similar to the expression that has been previously reported in *C. elegans*

(Korswagen, 2002). Expression is present predominantly in hypodermal cells, neurons in the ventral hypodermal region, and the vulval precursors and their progeny, persisting into L4 stage and adulthood (Seetharaman et al., 2010). Consistent with this expression pattern, examination of these GFP reporters at the adult stage showed that GFP expression is seen to localize to ectopic vulval protrusions in the *Cbr-pry-1(sy5353)* mutant background (Figure 10).

GFP expression levels were examined in the *C. briggsae* wild type and *sy5353* backgrounds at the late L1 stage, 10 hours after hatching. GFP expression was categorized as 'low' 'medium' or 'high' for each animal examined, and the distribution of expression levels was compared between the wild type and mutant backgrounds. While the *pry-1* mutant background appears to confer a higher variation in fluorescence levels than the more stable wild type background, both 2.4kb and 3.8kb *pry-1* 5' UTR GFP fusion expression appears to be heightened in the *Cbr-pry-1(sy5353)* mutant background, as indicated by a greater proportion of animals with 'high' levels of GFP expression (Figure 10). This result is consistent with our finding that *pry-1* expression is increased in *Cbr-pry-1(sy5353)* mutants when compared to wild type.

3.4 Summary and conclusions

This chapter discusses the finding that *pry-1/Axin* expression is responsive to Wnt signaling activity in both *C. elegans* and *C. briggsae.* This suggests that *pry-1* is itself a target of the very pathway in which it plays an integral regulatory

role. A potent negative regulator of Wnt signaling, positive regulation of *pry-1* expression by pathway activity indicates that feedback control is a key feature of Wnt signaling regulation in nematodes, as has been reported in vertebrate species including mouse and humans (Jho et al., 2002; Lustig et al., 2002; Yan et al., 2001). Thus, the mechanism of *pry-1/Axin* autoregulation appears to be evolutionarily conserved. While it is yet to be determined if *pry-1* is a direct transcriptional target of the Wnt pathway in these nematode species, the presence of conserved TCF/LEF TF POP-1 binding sites in its regulatory regions hints towards identification of *pry-1/Axin* as a bona fide target of the Wnt pathway in *C. elegans* and *C. briggsae*.

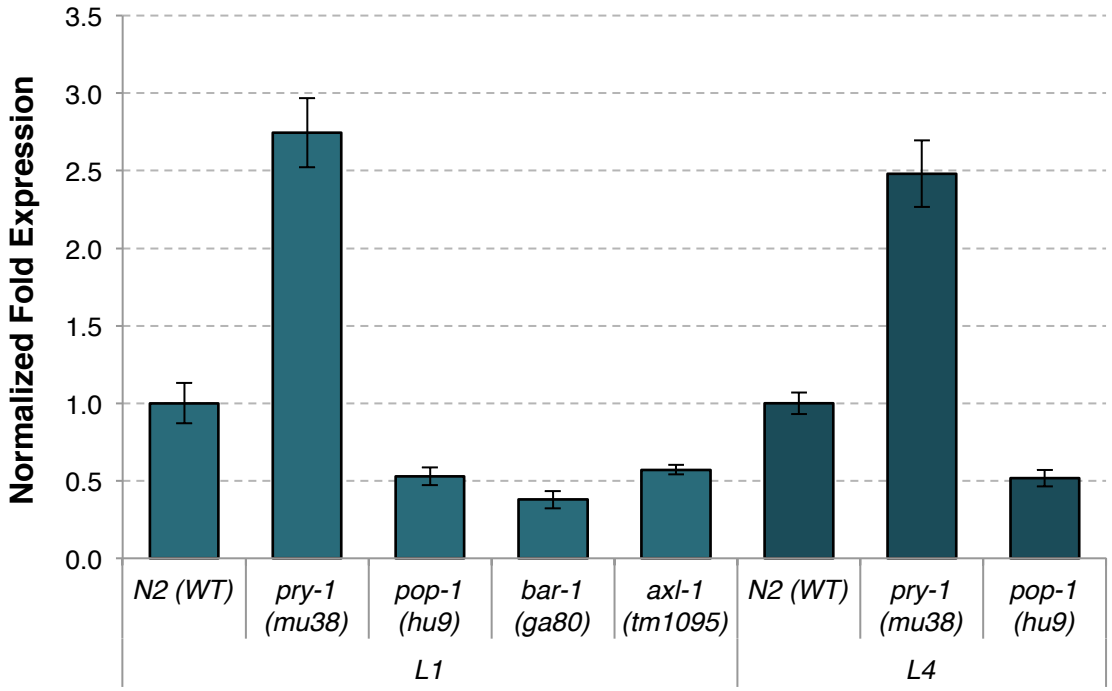

Figure 4. Fold changes in *pry-1* expression in *C. elegans* Wnt pathway mutants. L1 and L4 stage synchronized *C. elegans pry-1(mu38)* mutants show an increase in *pry-1* expression levels when compared to wild type N2. The opposite trend is observed when key positive regulators of Wnt pathway activity are knocked down (*bar-1/β-catenin* and *pop-1/TCF/LEF*), as well as the second Axin homolog in *C. elegans* (*axl-1)*. Fold expression is normalized to internal reference gene *pmp-3* in all trials. Error bars represent standard error of the mean ($p<0.05$ for all mutants compared to wild type).

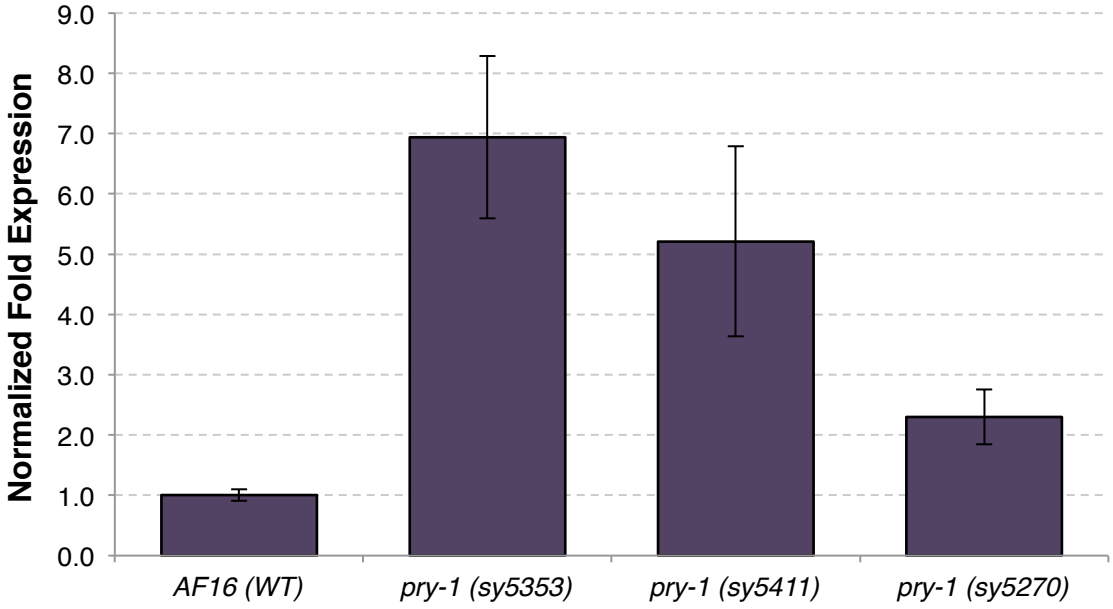

Figure 5. Fold changes in *Cbr-pry-1* expression in *Cbr-pry-1* mutant alleles. All alleles of *Cbr-pry-1* tested show an increase in the level of *Cbr-pry-1* in mixed stage populations. Fold expression is normalized to internal reference gene *Cbr-pmp-3* in all trials. Error bars represent standard error of the mean ($p<0.05$ for all alleles).

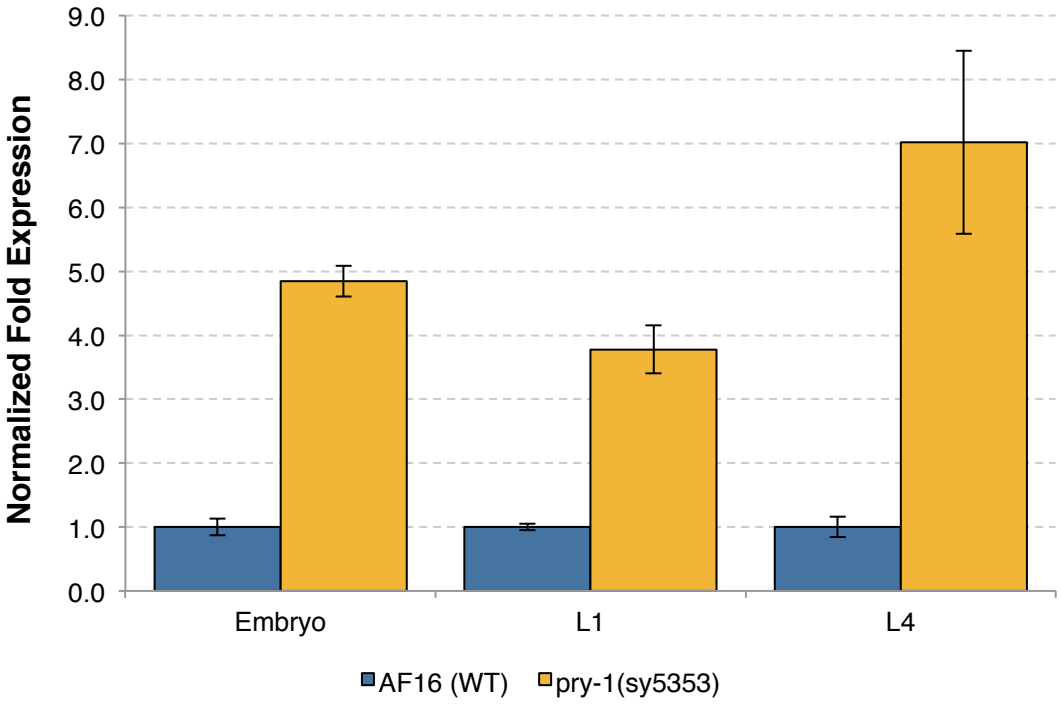

Figure 6. Cbr-*pry-1* levels across developmental stages in *C. briggsae pry-1 (sy5353)* mutants. *Cbr-pry-1* mutants exhibit an increase in *pry-1* transcript level compared to wild type AF16 at all developmental stages tested. Fold expression is normalized to internal reference gene *Cbr-pmp-3* in all trials. Error bars represent standard error of the mean ($p<0.05$ for all stages).

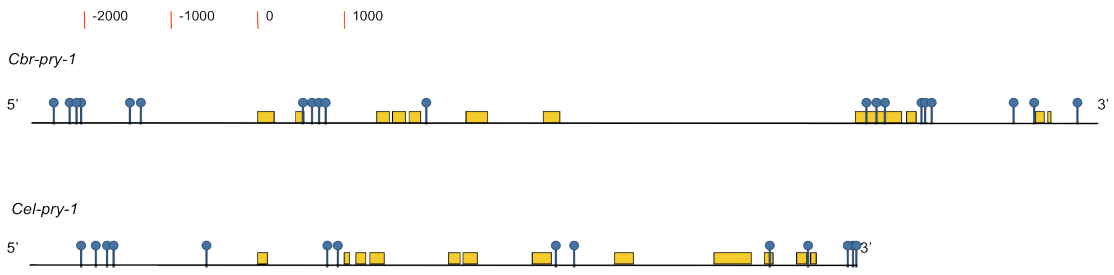

Figure 7. The *pry-1* UTR contains conserved TCF/LEF family transcription factor POP-1 binding sites in *C. elegans* and *C. briggsae*. The gene structure of *pry-1* in *C. briggsae* and *C. elegans* is shown. An analysis of *pry-1* UTRs using MatInspector indicates the presence of numerous conserved TCF/LEF family transcription factor POP-1 binding sites (YTTTGWW, indicated in blue), several of which are located within aligned regions of the gene.

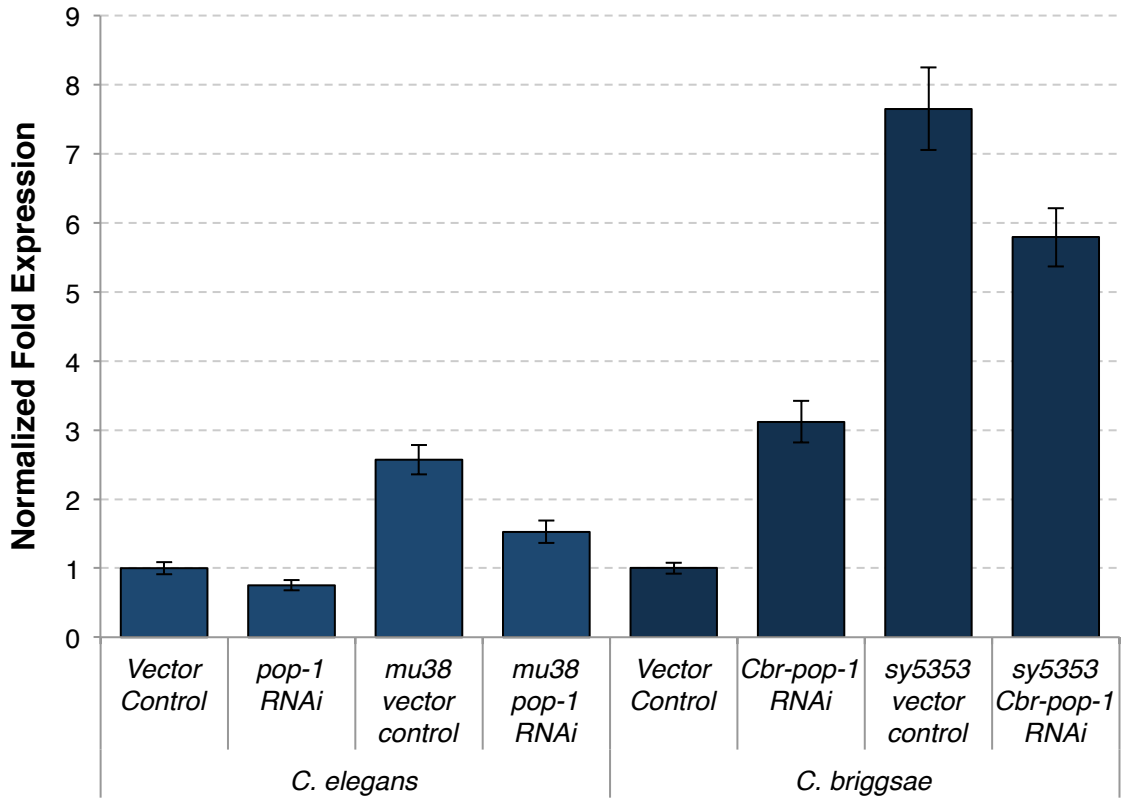

Figure 8. Effect of *pop-1* RNAi on *pry-1* and *Cbr-pry-1* expression levels. *C. elegans* and *C. briggsae* wild type and *pry-1* mutants (*'mu38'* and '*sy5353'*) were exposed to *pop-1* RNAi beginning at the L1 stage and collected at the L4 or young adult stage respectively for *pry-1* expression analysis by qRT-PCR. Fold expression is normalized to internal reference gene *pmp-3* or *Cbr-pmp-3* in all trials. Error bars represent standard error of the mean ($p<0.05$ for all conditions compared to their vector control).

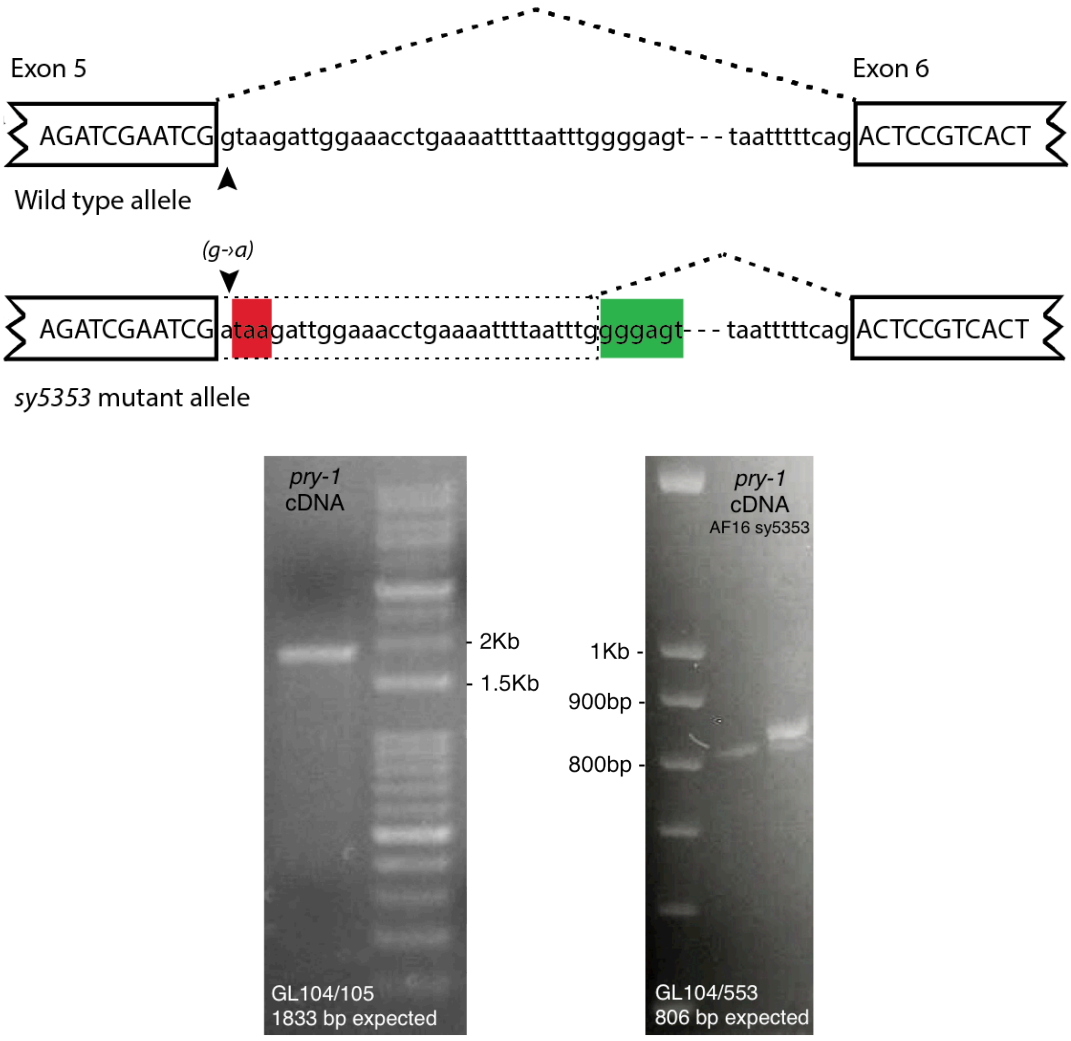

Figure 9. Sequencing of *Cbr-pry-1* cDNA in *Cbr-pry-1*(*sy5353)* mutants. Full length *Cbr-pry-1* cDNA sequence was amplified using primers GL104 and GL105 in the *Cbr-pry-1(sy5353)* mutant and sequenced. Splicing patterns of mRNA transcripts from wild type AF16 and *pry-1(sy5353)* mutant *pry-1* cDNA alleles are shown. In AF16, splicing occurs normally, exon 5 is spliced to exon 6. The sy5353 mutation is a G→A transition at the first base of intron 5 (arrows) that is predicted to disrupt the splicing donor site, introducing two in-frame stop codons within 40 bases. A 31 base portion of intron 5 appears to be included in the *sy5353* mutant *pry-1* cDNA sequence, which includes an in-frame stop codon, highlighted in red. Exon 6 sequence resumes at the point of a cryptic donor site within intron 5 closely resembling the 5' splice site consensus sequence GURAGU, highlighted in green. Sequencing primers GL104 and GL553 (Figure 3) were used for PCR to examine the sequence around the mutation site in wild type AF16 and the *Cbr-pry-1(sy5353)* mutant cDNA and confirm this finding. The expected wild type band size of 806bp was seen in both the wild type and mutant, however the *Cbr-pry-1* mutant showed an additional band approximately 30bp longer than the WT band, which agrees with the splicing error seen in the sequencing result.

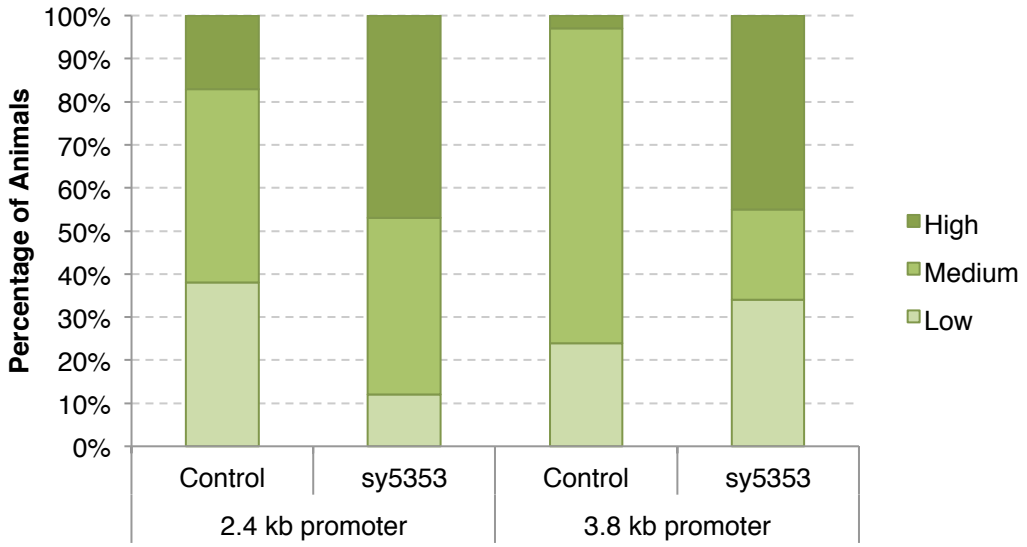
Percentage of Animals
100%
90%
80%
70%
60%
50%
40%
30%
20%
10%
0%
Control
sy5353
Control
sy5353
2.4 kb promoter
3.8 kb promoter
High
Medium
Low

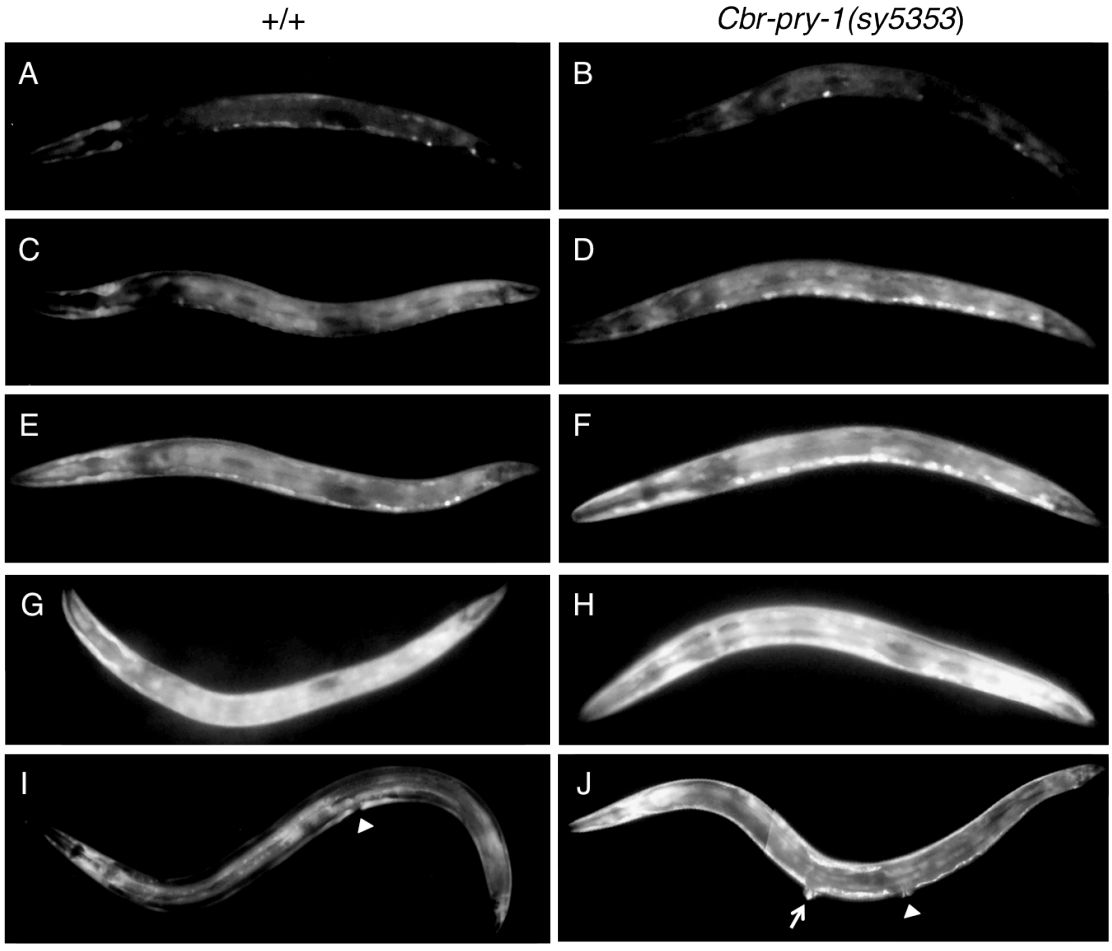
+/+
Cbr-pry-1(sy5353)
A
B
C
D
E
F
G
H
I
J

Figure 10. *Cbr-pry-1::GFP* transcriptional reporter expression in *C. briggsae*. Expression of transcriptional fusions of the *Cbr-pry-1* promoter region to GFP is visible throughout development in an array of cell types, predominantly in hypodermal cells, neurons in the ventral hypodermal region, and the vulval precursors and their progeny, persisting into the L4 stage and adulthood, where it localizes to ectopic vulval protrusions in *Cbr-pry-1(sy5353)* mutant animals (I-J, arrowhead indicates functional vulva, arrow indicates ectopic protrusion). GFP fluorescence level in 2.4kb and 3.8kb *pry-1* 5' UTR promoter fusions were examined in the wild type ('control', n=42 and 29 respectively), and *Cbr-pry-1(sy5353)* (n=34 and 29) backgrounds at the late L1 stage. GFP expression level was classified as 'low' (representative examples A-B), 'medium' (C-F), or 'high' (G-H) for each animal. It was found that in the *Cbr-pry-1(sy5353)* mutant background, while there is a wide variance in expression levels, the proportion of animals exhibiting 'high' levels of GFP expression increased when compared to the wild type control.

Chapter 4 – Genetic and Genomic Approaches to Wnt pathway target identification

4.1 Introduction

The Wnt signaling pathway is known to play a promiscuous role in nematode development, illustrated by its involvement in a wide variety of cellular and developmental processes. However, much is still unknown about the role and mechanism of action of the Wnt pathway in nematodes, and relatively few canonical Wnt pathway target genes have been identified. These known targets include *mab-5* (*Antennapedia/Ultrabithorax/ abdominal-A (Antp/Ubx/Abd-A) family*), *lin-39* (*Deformed/Sex combs reduced (Dfd/Scr*) *family*) *and egl-5* (*Abdominal-B (Abd- B) family*), three Hox genes that are involved in a variety of processes during nematode development. To gain a further understanding of the developmental role of Wnt signaling in the nematode, and the dynamics of Wnt pathway function, it is important to systematically identify the gene targets of the pathway. This will allow for the determination of novel processes linked to Wnt signaling, and a greater understanding of the regulation of these cellular processes by the conserved signal transduction pathways, including Wnt. Towards this goal of gene target identification in the nematode, we have undertaken both a genetic and genomics approach to identify known and novel targets of the Wnt signaling pathway in *C. elegans* and *C. briggsae*.

We have identified several hundred genes whose expression is altered in the Wnt pathway mutant background in both species. These genes could

potentially include transcriptional targets of the Wnt pathway. From within these Wnt responsive candidate genes, my focus has been on one prominent gene set which has been uncovered, that being the Hedgehog pathway related genes. In the traditional Hedgehog (Hh) signaling pathway, Hh acts as a ligand that binds to repress the Patched (Ptc) receptor, releasing the latent activity of membrane protein Smoothened (Smo), which is required for Hh signal transduction. This pathway is known to promote pattern formation and cell proliferation in *Drosophila* and vertebrates (Bürglin and Kuwabara, 2006). However, in *C. elegans,* the Hh pathway has undergone considerable evolutionary divergence. Homologs of Hh, Smo and other key pathway components are absent. Surprisingly, over sixty proteins referred to as the Hh-related proteins (WRT, GRD, GRL and QUA families), as well as PTC, and PTC-related (PTR) proteins are present (Bürglin and Kuwabara, 2006). A global survey of the phenotypes produced by RNA-mediated interference (RNAi) for the PTC, PTR and Hh-related genes indicated that they play multiple roles in *C. elegans* development*,* including a key role in molting, the shedding of the cuticle (exoskeleton) that is synthesized at each larval stage during development to allow for growth. The function of these proteins appears to be conserved between *C. elegans* and *C. briggsae* (Zugasti et al., 2005). A description of our search for these candidate Wnt target genes using parallel genetic and genomics approaches follows.

4.2 A forward genetic approach to Wnt pathway target identification: *pry-1* mutant phenotype suppressor analysis in *C. briggsae*

An EMS mutant screen in *Cbr-pry-1(sy5353)* was previously carried out in our lab by Bavithra Thillainathan to identify modifiers of the *pry-1* mutant Multivulva phenotype. This screen focused on the vulva phenotype specifically as Wnt signaling is known to be required for proper development of the vulva, and vulval phenotypes are amenable to rapid visual screening. The goal of this screen was to both identify novel downstream gene targets of the Wnt pathway as well as to isolate mutants of additional Wnt pathway components in *C. briggsae*, as *Cbr-pry-1* is the only Wnt pathway mutant available in this nematode species at this time. The isolation of *C. briggsae* Wnt mutants would aid in comparative analysis of Wnt pathway regulation and function in *C. elegans* and *C. briggsae.*

Many promising mutants were isolated, and we began our study with the two strains showing the strongest suppression of the Multivulva phenotype in the *pry-1 (sy5353)* background. Strains 4B and 51D were isolated in this screen and exhibited significant suppression of the Muv phenotype (10% Muv, n=31 and 7% Muv, n=31, respectively) in comparison to the mutagenized *Cbr-pry-1(sy5353)* strain (94% Muv, n=66). Each of these strains have been outcrossed 2x to the parental strain to eliminate unwanted secondary mutations prior to analysis. These outcrossed suppressor strains retained suppression of the Muv phenotype, though Muv penetrance increased in both 4B (41% Muv, n=104) and 51D (42% Muv, n=134). Using insertion-deletion (indel) as well as SNP-Chip polymorphism

mapping techniques, the chromosomal location of these suppressor mutations has been characterized, facilitating a search for candidate genes.

The mapping cross used for polymorphism based mapping is shown in Figure 11. Briefly, one must cross hermaphrodites of the mutant strain in the AF16 reference strain background to males of the mapping polymorphic strain (HK104). As our suppressor mutants were isolated, and must remain in a *pry-1(sy5353)* mutant background for their phenotype to be recognizable, a 10x introgression of the AF16-type *sy5353* locus into the HK104 background was completed by Bavithra Thallainathan. This was used as the "mapping strain". Additionally, as *sy5353* males are unable to mate efficiently, the 10x introgressed *sy5353* line in the HK104 background was initially crossed to a GFP expressing HK104 so that the resulting *sy5353/+* males could be used in this mapping cross. In the F1 generation, Muv heterozygous cross progeny were allowed to self fertilize, allowing recombination to occur amongst the AF16 and HK104-type chromosomes. In the F2 generation, 10 hermaphrodite worms that show suppression of the Muv phenotype (are phenotypically non-Muv) are pooled, genomic DNA is extracted from these worms, and the ratio of AF16 and HK104 type DNA at each polymorphism marker is observed using agarose gel electrophoresis. Unlinked markers (polymorphic loci) will be comprised of equal proportions of the AF16 and HK104 type DNA. A higher ratio of AF16 DNA at a particular marker indicates the mutation has linkage to this marker. Once linked to

a chromosome, the location of the *C. briggsae* gene mutation can be further refined to a chromosomal region using additional polymorphisms or a SNP-Chip mapping approach. From here, identification of candidate genes located in this region followed by deep sequencing of the genomic interval of interest to identify mutations that disrupt open reading frames can allow you to identify the affected gene. Additional analysis such as comparison to the *C. elegans* annotation can reveal if the mutant gene is conserved between these nematode species or is a novel *C. briggsae* gene.

4.2.1 Mapping of 4B

Suppressor strain 4B was mapped to chromosome 4 using an insertion-deletion polymorphism (indel) mapping technique. One medium indel marker located close to the center of each chromosome was used to determine linkage as described in Figure 12. A higher ratio of AF16-type DNA is seen at the chromosome 4 marker when compared to DNA extracted from heterozygous F1 worms with equal proportions of AF16 and HK104- type DNA. Confirmation of this linkage was performed using snip-SNP polymorphism cb48850 which disrupts a HindIII restriction enzyme binding site located near the center of chromosome 4 (see Figure 12, Koboldt et al., 2010). Having narrowed the search for the suppressor gene to the chromosome level, finer mapping techniques will be used to elucidate the precise chromosomal location of the affected gene, allowing for further analysis and identification of the gene containing this *Cbr-pry-1* mutant

suppressor mutation.

4.2.2 Mapping of 51D

SNP-Chip mapping uses a SNP-based oligonucleotide microarray containing 9701 well spaced SNPs across each of the chromosomes to identify and precisely map *C. briggsae* mutants (Zhao et al., 2010). Preparation of a strain for SNP-Chip mapping is similar to the mapping cross used for indel mapping (Figure 11), however 100 F2 worms are picked and allowed to reproduce for several generations before the genomic DNA is extracted for hybridization to the SNP-Chip. Differences in the hybridization signals between oligos of the array from AF16 and HK104 can be detected. Based on the intensity and the arc of the mapping signal produced, approximate chromosomal position of the mutation can be determined, aiding in mutant gene identification (Zhao et al., 2010).

Suppressor 51D was determined to have a mutation in the right arm of Chromosome 1, in a similar location to that of the *Cbr-pry-1(sy5353)* mutation itself (seen in Figure 13). The *Cbr-pry-1* locus was sequenced around the mutation site in the 2x outcrossed 51D suppressor strain to determine if this suppressor mutation is a revertant of the *Cbr-pry-1(sy5353)* mutation. However, we found that the original *sy5353* mutation is still intact in the suppressor strain. It is possible that the suppressor mutation is a second site revertant within the *Cbr-pry-1* gene or an additional mutation in a gene of a similar chromosomal location

to *Cbr-pry-1.* Further sequencing of the entire *Cbr-pry-1* locus in suppressor strain 51D will clarify the nature of this suppressor mutation.

With further characterization of these, along with the many other Muv suppressor mutants isolated in the EMS screen, we hope to both identify novel genetic targets of the Wnt pathway in *C. briggsae,* and identify mutations in known or novel Wnt pathway components that can be used for further study of Wnt signaling in *C. briggsae.*

4.3 A Comparative Transcriptomics Approach to Wnt Pathway Target Identification

4.3.1 Justification and experimental setup

Another approach for the study of Wnt pathway regulation and function is through genome-wide identification of target genes whose transcription is regulated in response to Wnt pathway activity. Very few canonical Wnt pathway target genes have been identified in *C. elegans* and *C. briggsae* thus far. Therefore, to further dissect the role of the Wnt pathway in conserved signaling networks and developmental processes we have taken a comparative transcriptomics approach using Whole Transcriptome Shotgun Sequencing (RNA-seq) to search for novel transcriptional targets of the Wnt pathway in *C. elegans* and *C. briggsae* (Wang et al., 2009). Using this system we can perform a gene expression analysis for both mRNA and miRNA targets, examining and comparing the regulation of gene transcription in response to Wnt pathway activity in both species.

For this comparison of gene expression in response to Wnt signaling activity, we have performed RNA-seq experiments on larval L1 stage synchronized worms from wild type and *pry-1* mutants of each species: *C. elegans* N2 and *pry-1(mu38),* and *C. briggsae* AF16 and *pry-1(sy5353).* The L1 stage was chosen for our analysis as Wnt signaling is highly active at this stage, as indicated by the high expression levels of Wnt pathway signaling components (Figure 14, Hillier et al., 2009). Another advantage of analysis in the L1 stage is that it allows for relative ease of achieving a high degree of developmental synchrony between the wild type and mutant worm populations. To obtain tightly synchronized animals, two consecutive rounds of bleach synchronization were performed on large-scale cultures of gravid hermaphrodites of each genotype. In the final round, hermaphrodites were bleached 6 hours after the first egg was laid on the plates. The resulting embryos obtained were allowed to age on agar plates without any OP50 bacteria at 20°C for 16 hours, and whole worms were then collected in M9 buffer for RNA extraction and processing. Two independent extractions were performed for each genotype, to be sent as duplicates for sequencing. Quantification and analysis using an Agilent 2100 Bioanalyzer were performed on each sample to ensure the RNA was of the highest quality and integrity. After RNA extraction and quality assessment, each sample was sent to the Génome Québec Innovation Centre, where cDNA libraries enriched for the mRNA and miRNA portions of each sample were prepared and high throughput

sequencing was performed on an Illumina HiSeq 2000. The resulting sequence reads were aligned to the reference genome of each species (UCSC ce6 in *C. elegans* and CB3 in *C. briggsae)* and bioinformatics analysis was performed by Ayush Ranawade using the Bowtie-express aligner coupled with DEseq for differential gene expression analysis, to elucidate those mRNA and miRNA genes from each species that show a significant change in expression between the wild type and Wnt pathway overactive *pry-1* mutants.

4.3.2 Differentially expressed gene targets in *C. elegans* and *C. briggsae*

Our RNA-seq analysis returned hundreds of diverse candidate target genes that are differentially expressed in both *C. elegans* and *C. briggsae*. A global view of these targets is presented and described in Figure 15. For our initial experiments, we decided to classify the function of each gene target based on their associated Gene Ontology (GO) terms, and focus on two defined sets of targets that exhibit differential expression between wild type and *pry-1* mutant backgrounds in both species. We observed that while there are significant differences in the individual genes that are differentially expressed in *C. elegans* and *C. briggsae,* many gene families are highly represented in both species.

While a vast assortment of candidate target genes were returned in our analysis, ranging from vulval transcription factors to genes required for neuronal differentiation and axon migration, we have isolated two gene sets to pursue. The first being those genes involved in aging processes, and secondly, those genes

related to Hedgehog pathway function in nematodes. Those genes involved in life span and aging, including the miRNA targets, have been validated and analyzed by Ayush Ranawade, while genes related to Hedgehog pathway function are my focus of study. As the primary known role of the Hh pathway in nematodes is in molting, we are also interested in investigating additional Wnt pathway target genes that have been shown to share this role in molting and cuticle development but are not necessarily known to be related to the Hh pathway (Frand et al., 2005).

We chose to initially filter our targets by selecting those that exhibit a fold change in expression of >1.5 in either direction on a $\log_2$ scale and an adjusted p-value ≤ 0.05 in the *pry-1* mutant compared to wild type. A list of those differentially expressed target genes involved in the Hedgehog pathway, or molting and cuticle development more generally, can be seen in Table 3 (*C. elegans)* and Table 4 *(C. briggsae).* Several of these candidate target genes are shared between the two species, including Hedgehog pathway genes *grd-12, grl-5, grl-7, grl-16, ptr-16,* and *ptr-19* (indicated in Table 3). Many of the additional top targets on the candidate target gene lists for both species are Hedgehog pathway genes as well. These include Hedgehog-related (*grl* and *wrt*) genes and Patched-related (*ptr*) genes in *C. briggsae,* and Hedgehog-related (*grd, grl*)*,* as well as Patched-related (*ptr*) genes in *C. elegans.* The *C. elegans* target gene set also includes *phg-1,* which encodes the ortholog of human signaling modulator glycoprotein

Gas1 (Bürglin, 2006). As for those genes involved in molting and cuticle development more generally, the *C. briggsae* gene set includes 18 genes, while the *C. elegans* gene set contains only 3, with one of these genes (*rol-6*) being shared between the two species. Interestingly, though Wnt signaling activity is up regulated in our *pry-1* mutants, all of the Hh and molting related candidate target genes that met our threshold are down regulated in *pry-1* mutants in both species compared to wild type.

To further refine this gene list for our initial experiments, those gene targets with a >2 fold change in expression that are linked to the Hedgehog pathway in *C. elegans* were selected for initial validation of RNA-seq results using qRT-PCR. These genes include Patched-related family genes *ptr-16, ptr-19* and *ptr-20,* groundhog (Hedgehog-like family) genes *grd-14, grd-15* and *grd-6* and ground-like (grd-related) genes *grl-1, grl-16, grl-21, grl-4, grl-6* and *grl-13.*

Additionally, it is notable that we found *pry-1* itself to be identified as a target, showing a significant increase in expression in both the *C. elegans* and *C. briggsae pry-1* mutants compared to wild type. This confirms our previous qRT-PCR results described in Chapter 3 and gave us confidence in our methods of target identification.

4.3.3 Validation of Hedgehog pathway related Wnt pathway gene targets

The candidate target genes that have been identified in our RNA-seq experiments must be validated using qRT-PCR for confirmation. For these initial

experiments we have primarily focused on the targets identified in *C. elegans,* due to the ease of subsequent functional studies, as there is an abundance of available reagents and tools for this species as compared to *C. briggsae*. Primer sets for each of the 12 Hedgehog pathway related genes exhibiting a $\log_2$fold change in expression > 2 in the *pry-1* mutant were designed and validated for efficiency of amplification in qRT-PCR experiments. Total RNA was extracted from synchronized L1 stage wild type N2 and *pry-1(mu38)* worms following the same protocol as was used previously for the RNA-seq analysis. cDNA was then synthesized from these samples for qRT-PCR amplification of our target genes in an attempt to recapitulate the observed RNA-seq results.

We were unable to reliably validate several of the candidate gene targets (*grl-13, ptr-16* and *ptr-20*) due to difficulties performing qRT-PCR experiments on those genes with very low abundance at the L1 stage (Hillier et al., 2009). Of those targets we were able to successfully analyze, we found 8 genes that followed the same trend in expression seen in our RNA-seq analysis, though the fold changes varied compared to the RNA-seq results. Hedgehog pathway genes *grd-6, grd-14, grd-15, grl-4, grl-6, grl-16, grl-21* and *ptr-19* display significantly reduced expression in the pry-1*(mu38)* mutant background compared to wild type (0.39, 0.19, 0.11, 0.09, 0.01, 0.12, 0.02 and 0.41 fold expression respectively, Figure 16). One gene, *grl-1,* did not exhibit a significant difference in expression between the *pry-1* mutant and wild type backgrounds (0.81 fold expression in *pry-*

1(mu38), Figure 16). Further validation of additional mRNA targets in both *C. elegans* and *C. briggsae* such as those presented in Tables 3 and 4 will allow us to develop a greater understanding of the extent of accuracy of our RNA-seq results.

4.3.4 Molting and cuticle defects in *C. elegans* and *C. briggsae pry-1* mutants.

We have found the Hedgehog gene family featured prominently in our analysis of Wnt pathway responsive gene targets in both *C. elegans* and *C. briggsae*. As the nematode incarnation of Hedgehog signaling is known to play an important role in the developmental control of molting processes, and several other molting-related gene targets were identified in our analysis, this led us to perform a preliminary screen and interspecies comparison of any defects in molting and cuticle development in the *pry-1* mutants. The adult stage was chosen for observation based on previous findings that knockdown of Patched and Hedgehog-related homologs in *C. elegans* by RNAi most commonly results in molting and cuticle defects at the L4-Adult stage molt (Zugasti et al., 2005).

A previously unreported 'roller' defect was found in the *C. elegans pry-1(mu38)* mutant (32% penetrance, n=31), in which the wild type sinusoidal wave pattern of nematode movement is disrupted and the body of the animal rotates along its long axis when in motion, causing it to move in a corkscrew pattern (Brenner, 1974). Roller phenotypes are characteristic of several of our target

genes, most notably *rol-6*, which encodes a cuticle collagen which is required for normal cuticular morphology, and was identified as exhibiting significantly reduced expression in both *C. elegans* and *C. briggsae pry-1* mutants in our RNA-seq analysis (Tables 3 and 4, Kramer et al., 1990). Roller phenotypes are characteristic of defective cuticle morphology, and are often the result of defective alae. Alae are ridge-like specialized cuticular structures, formed by the terminal differentiation of the epithelial seam cells after their final division at the L4 stage, that allow the worm to move in a stable manner throughout its environment (Sulston and Horvitz, 1977). Alae morphology defects are a common phenotype seen upon elimination of *ptr* or *hh*-r gene activity by RNAi in *C. elegans,* including some of those genes found to be downregulated in the *pry-1* mutants in our RNA-seq analysis such as *ptr-20* and *ptr-1* in *C. elegans* and *wrt-1, wrt-4,* and *wrt-7* in *C. briggsae* (Tables 3 and 4, Zugasti et al., 2005). We found evidence of alae defects in both *C. elegans* and *C. briggsae pry-1* mutants (Figure 17). In *mu38* mutants, the alae appear severely malformed, with the lateral alae displaying a fragmented “beaded” appearance. In *Cbr-pry-1(sy5353)* mutants, no roller phenotype was detected (0% penetrance, n=30), and alae defects seen in these worms are less severe, typically featuring breaks in the alae (Figure 17). Other varied molting defects such as blisters in the cuticle were seen in *C. briggsae pry-1* mutants (Figure 17). Further characterization of these phenotypes and their penetrance within Wnt pathway component mutant populations will allow for a

greater understanding of the significance of these defects, and may provide support for an interaction between the Wnt and Hedgehog pathways.

4.4 Summary and conclusions

This chapter has chronicled our search for gene targets of the Wnt signaling pathway in *C. elegans* and *C. briggsae* using both genetic and genomics approaches. While much of this work is ongoing, we have uncovered a novel interaction between the Wnt and Hedgehog signaling pathways in both nematode species. It is likely that with further characterization of the Wnt target genes elucidated in both the forward genetic suppressor screen and the transcriptome sequencing project, additional pathway interactions and bona fide targets of the Wnt pathway will be exposed.

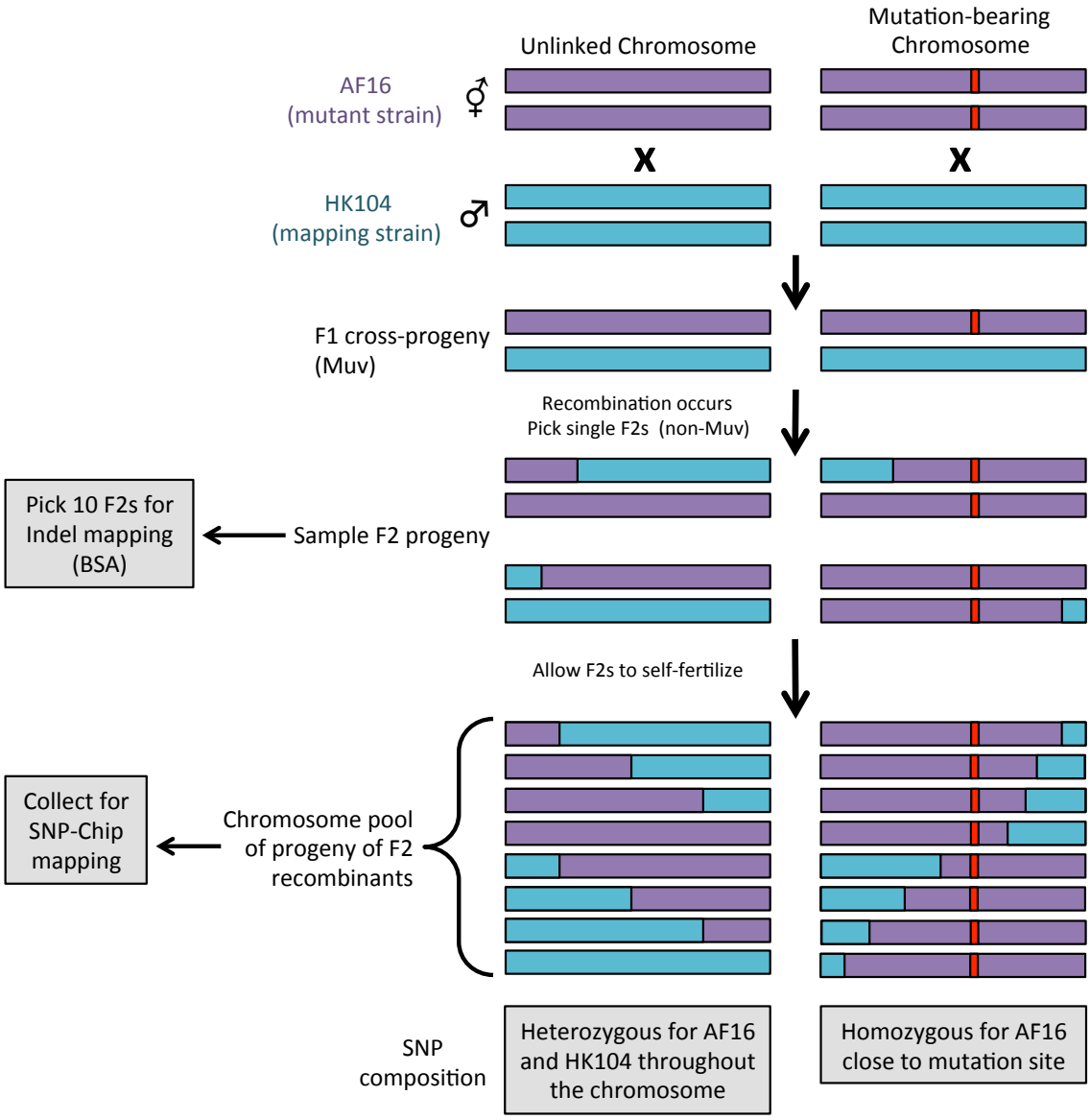

Figure 11. Mapping cross scheme for polymorphism based mapping in *C. briggsae* (Adapted from Boulin & Hobert, 2012).

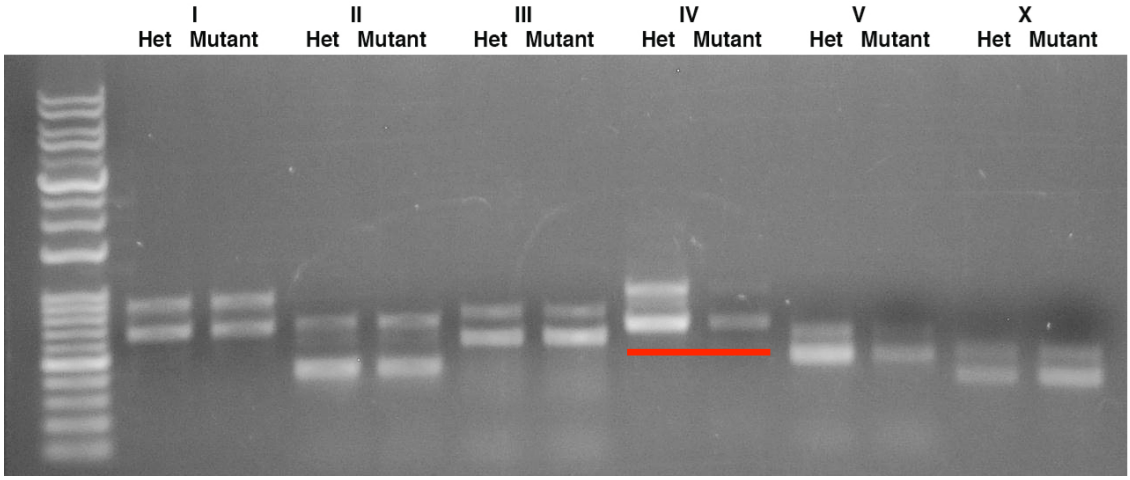

Chromosome	Indel ID	Indel Type
1	cb-m142	250bp Insertion in HK104
2	cb-m26	290bp Deletion in HK104
3	cb-m46	270bp Deletion in HK104
4	cb-m172	250bp Insertion in HK104
5	cb-m103	200bp Deletion in HK104
X	cb-m127	195 bp Deletion in HK104

Chromosome	snip-SNP ID	Expected bands
4	cb48850	Disrupts HindIII site → 750bp band in AF16 → 314bp and 436bp bands in HK104

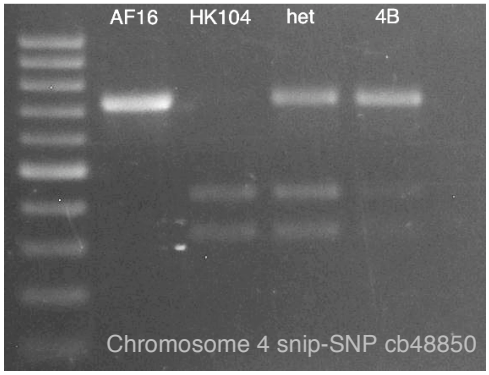

Figure 12. Mapping of *Cbr-pry-1* Muv phenotype suppressor mutation in strain 4B. The *Cbr-pry-1(sy5353)* phenotype suppressor mutant 4B was mapped using medium indel polymorphism markers and shows linkage to chromosome 4. Confirmation of this linkage was performed using a chromosome 4 snip-SNP polymorphism that disrupts a restriction enzyme recognition site. The indel markers used for each chromosome are listed (Koboldt et al., 2010). 'Het' refers to DNA containing equal parts AF16 and HK104 extracted from the F1 generation of the mapping cross (See Figure 11).

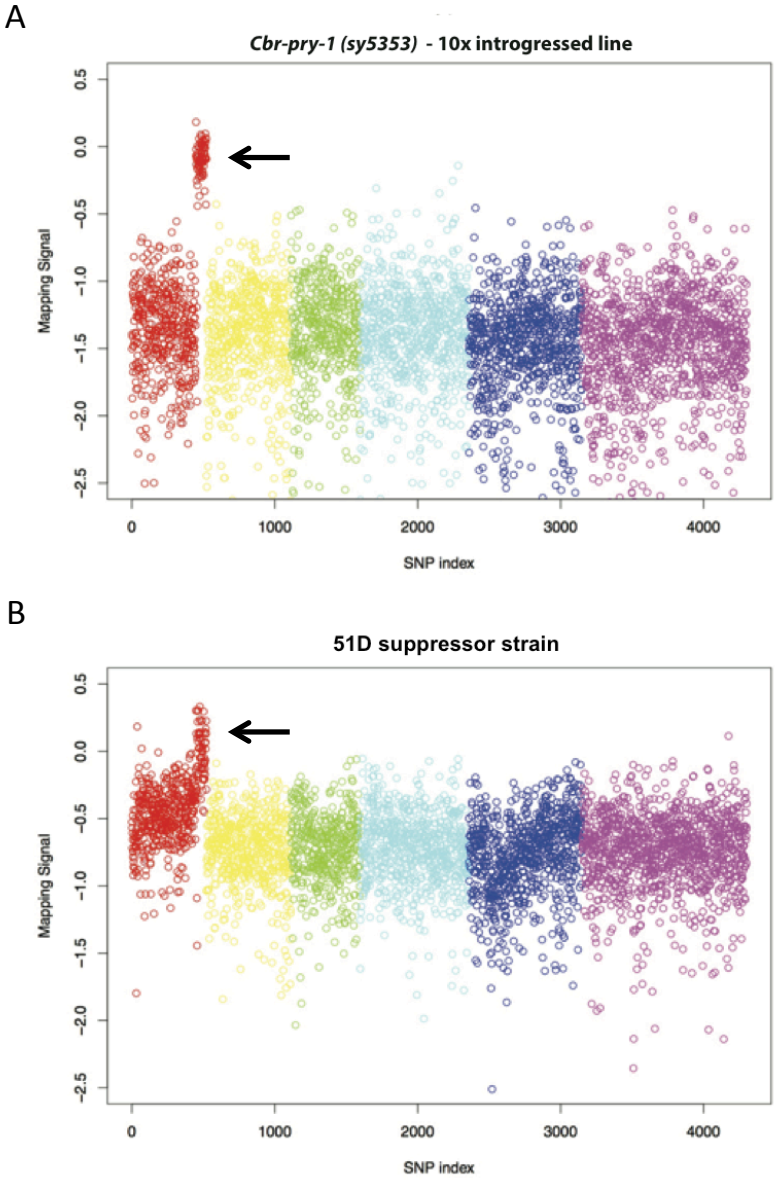

Figure 13. SNP-Chip mapping of suppressor mutation in strain 51D. Mapping signal is plotted against the SNP index along the six colour coded chromosomes from 1 to 5 and X. Differences in the hybridization signals between oligos of the array from AF16 and HK104 are detected. A mapping signal towards the positive end of the spectrum represents those oligonucleotides that are predominantly AF16-type, indicating the location of the mutation that is being mapped (Zhao et al., 2010). The suppressor mutation in 51D, represented by a higher ratio of AF16-type signal, was localized to the right arm of Chromosome 1 (arrow in B), in a similar location to the AF16-type *pry-1* locus in the *Cbr-pry-1(sy5353)* 10x introgressed HK104 background mapping strain (arrow in A). Each SNP is represented on the array by a single dot.

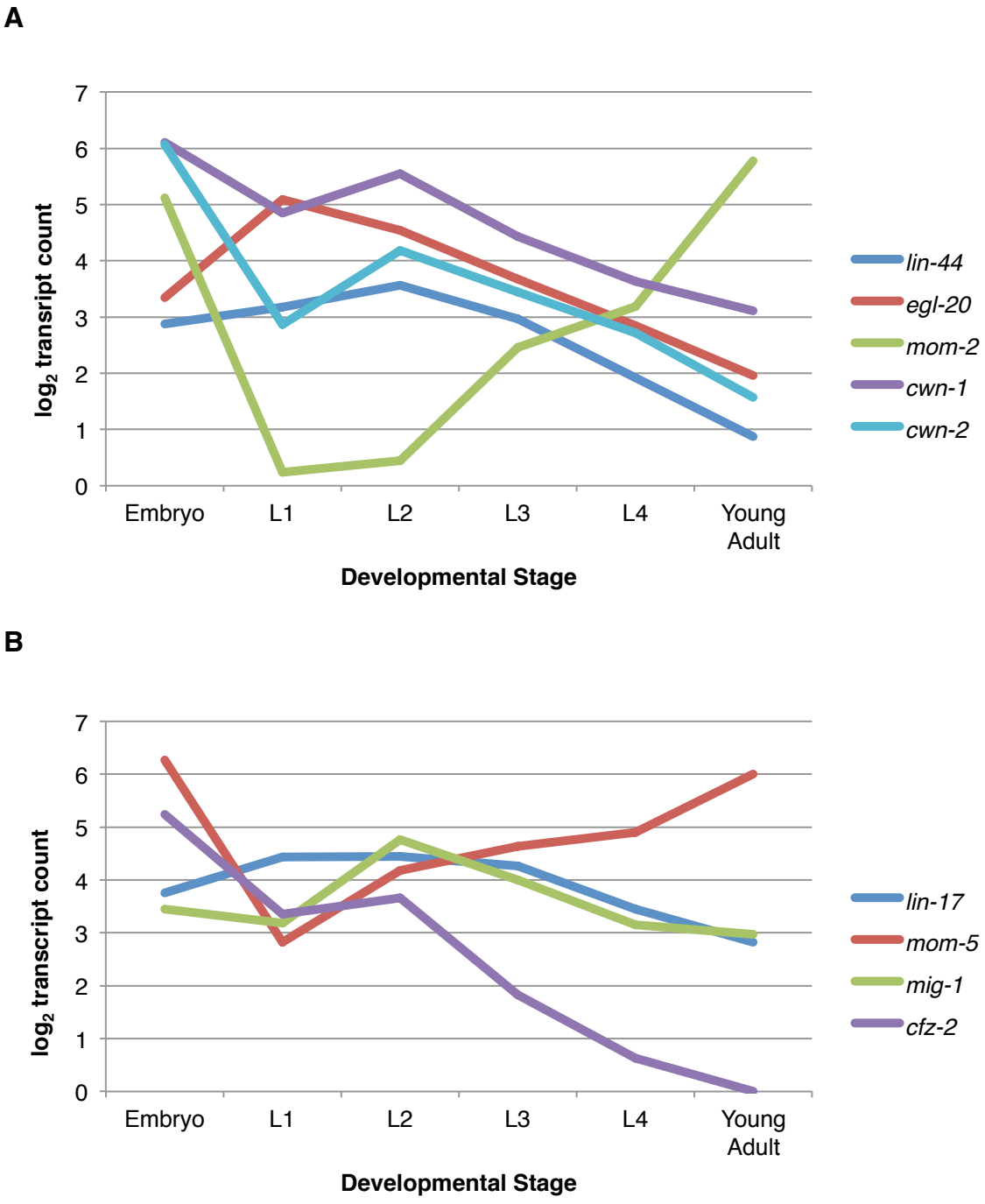

Figure 14. Developmental time course of *C. elegans* Wnt pathway ligand and receptor expression. L1 stage expression is high in the majority of *C.elegans* Wnt pathway ligands (A) and receptors (B) (Based on RNA-seq data from Hillier et al., 2009).

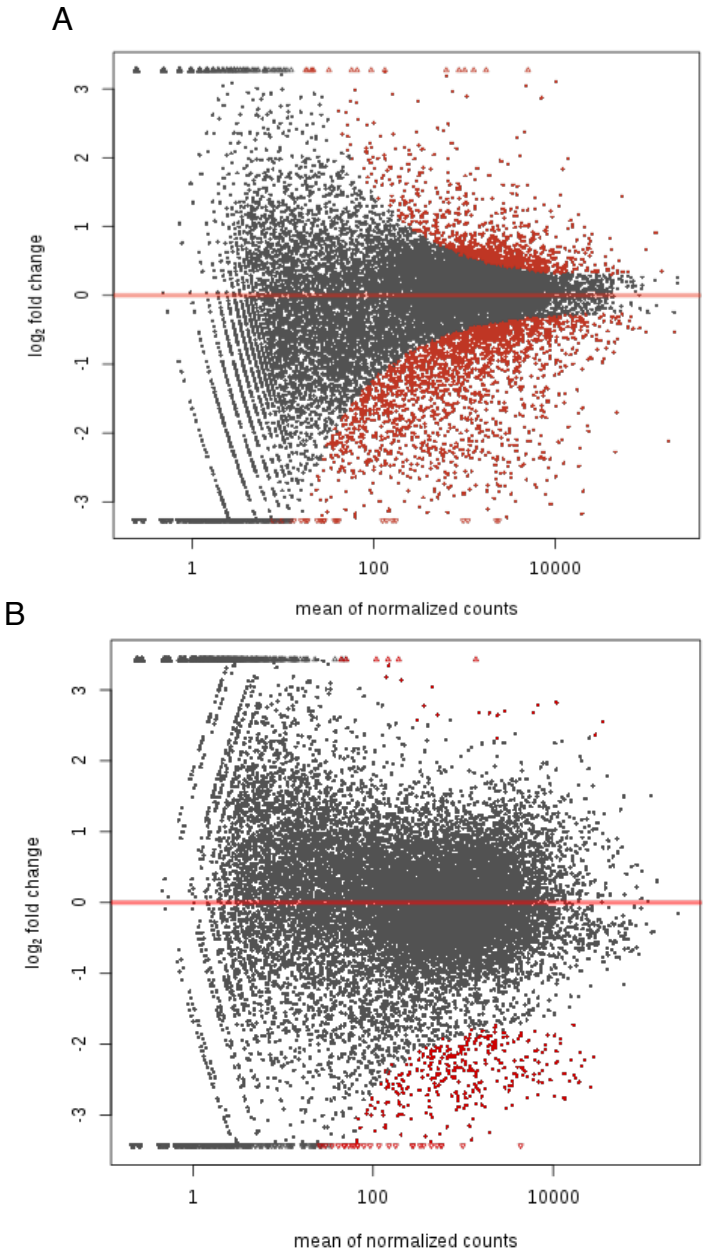

Figure 15. MA plots of *C. elegans* and *C. briggsae* RNA-seq results. Represented is the $\log_2$ fold change comparing transcripts derived from animals exposed to over-activation of Wnt pathway (*pry-1* mutants) versus wild-type activation in *C. elegans* (A) and *C. briggsae* (B). Each point represents an individual gene. Data points above 0 represent up-regulated genes, while data points below 0 represent down-regulated genes. Red data points represent those points meeting the criteria of adjusted p-value < 0.05, totaling 2660 genes in *C. elegans* and 271 genes in *C. briggsae.* Plots were created using the DEseq package.

Table 3. Hedgehog pathway and molting-related gene targets in *C. elegans.*

Gene ID	Fold Change	log_2 Fold Change	*C. briggsae* Match
grl-16	0.169	-2.566	*
grd-15	0.181	-2.466	
ptr-16	0.197	-2.347	*
tag-297	0.199	-2.326	
grl-6	0.202	-2.308	
grd-6	0.202	-2.305	
grd-14	0.205	-2.283	
grl-1	0.215	-2.216	
ptr-20	0.221	-2.180	
grl-4	0.225	-2.154	
ptr-19	0.227	-2.137	*
grl-21	0.230	-2.120	
grl-13	0.233	-2.102	
bli-5	0.252	-1.988	
grl-5	0.264	-1.920	*
rol-6	0.287	-1.802	*
grl-7	0.290	-1.788	*
phg-1	0.304	-1.718	
ptr-22	0.316	-1.662	
grd-12	0.337	-1.569	*
ptr-1	0.341	-1.551	

Top Hedgehog pathway and molting-related genes exhibiting >1.5 log_2 fold change in expression in *pry-1(mu38)* mutants compared to wild type N2 in *C. elegans* are listed. Blue highlighting indicates genes involved in the Hedgehog pathway. Those genes which also show a significant differential expression in the *C. briggsae* data set are indicated with an asterisk. p_{adj} <0.01 for all genes.

Table 4. Hedgehog pathway and molting-related gene targets in *C. briggsae*

Gene ID	Fold Change	log_2 Fold Change	Gene ID	Fold Change	log_2 Fold Change
Cbr-grl-15	0.120	-3.054	*Cbr-fkb-5*	0.194	-2.363
Cbr-grl-5	0.138	-2.855	*Cbr-wrt-4*	0.198	-2.336
Cbr-glf-1	0.146	-2.774	*Cbr-elo-5*	0.205	-2.285
Cbr-rol-6	0.148	-2.754	*Cbr-ptr-18*	0.213	-2.231
Cbr-wrt-1	0.149	-2.749	*Cbr-noah-2*	0.214	-2.221
Cbr-grl-2	0.162	-2.626	*Cbr-dpy-3*	0.220	-2.184
Cbr-bus-8	0.163	-2.619	*Cbr-noah-1*	0.221	-2.176
Cbr-cuti-1	0.172	-2.541	*Cbr-hhat-1*	0.229	-2.127
Cbr-wrt-10	0.173	-2.531	*Cbr-ptr-16*	0.229	-2.125
Cbr-mltn-9	0.179	-2.483	*Cbr-mlt-11*	0.230	-2.119
Cbr-wrt-2	0.179	-2.482	*Cbr-ptr-4*	0.232	-2.107
Cbr-wrt-6	0.180	-2.473	*Cbr-acn-1*	0.237	-2.078
Cbr-grl-7	0.187	-2.421	*Cbr-ptr-19*	0.237	-2.076
Cbr-mlt-8	0.187	-2.419	*Cbr-nas-37*	0.243	-2.040
Cbr-grl-16	0.187	-2.419	*CBG19137*	0.249	-2.007
Cbr-ptr-2	0.193	-2.375	*CBG23138*	0.252	-1.991
Cbr-mlt-9	0.194	-2.366			

Top Hedgehog pathway and molting-related gene targets showing >1.5 fold change in expression in *pry-1(sy5353)* mutants compared to wild type AF16 in *C. briggsae* are listed**.** Blue highlighting indicates genes involved in the Hedgehog pathway. $p_{adj} \leq 0.05$ for all genes.

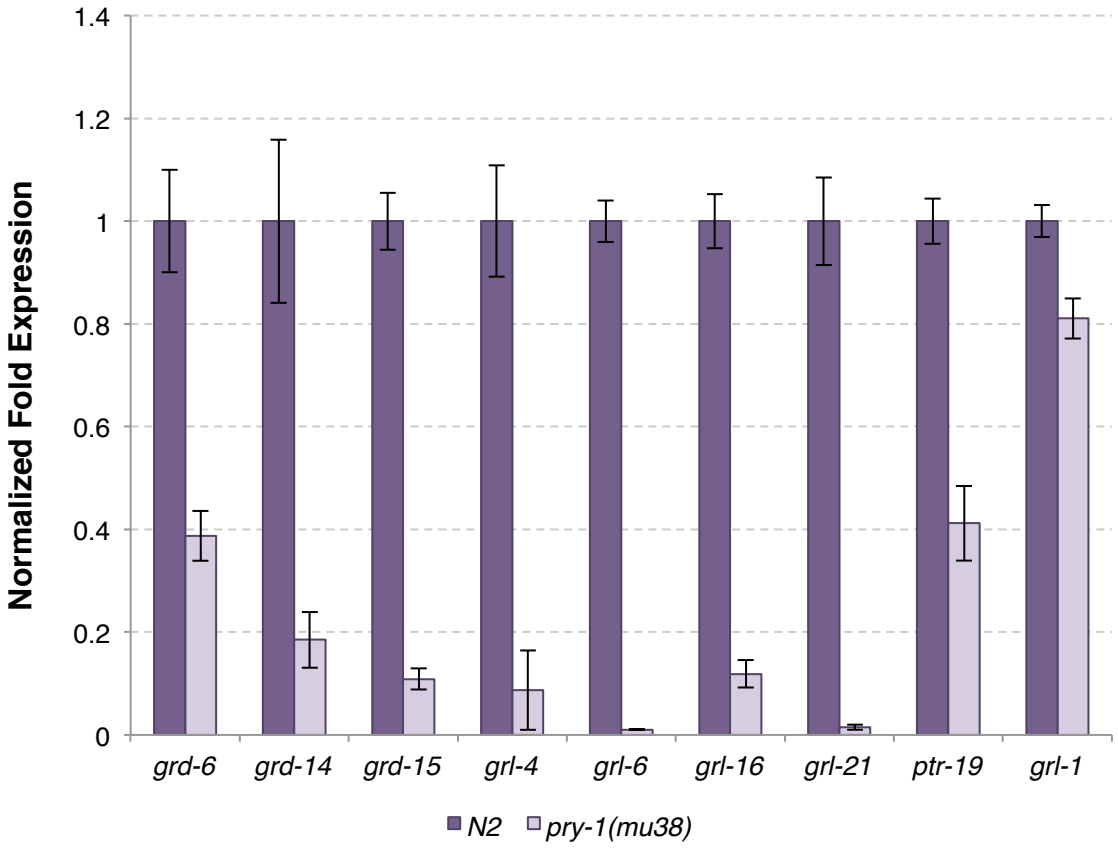

Figure 16. qRT-PCR validation of *C. elegans* Wnt pathway targets identified in RNA-seq analysis. All genes tested show a decrease in expression in the *pry-1(mu38)* mutant background. All trials are normalized to internal reference gene *pmp-3*. Error bars represent standard error of the mean. $p < 0.01$ for all genes except *grl-1* (p=0.023).

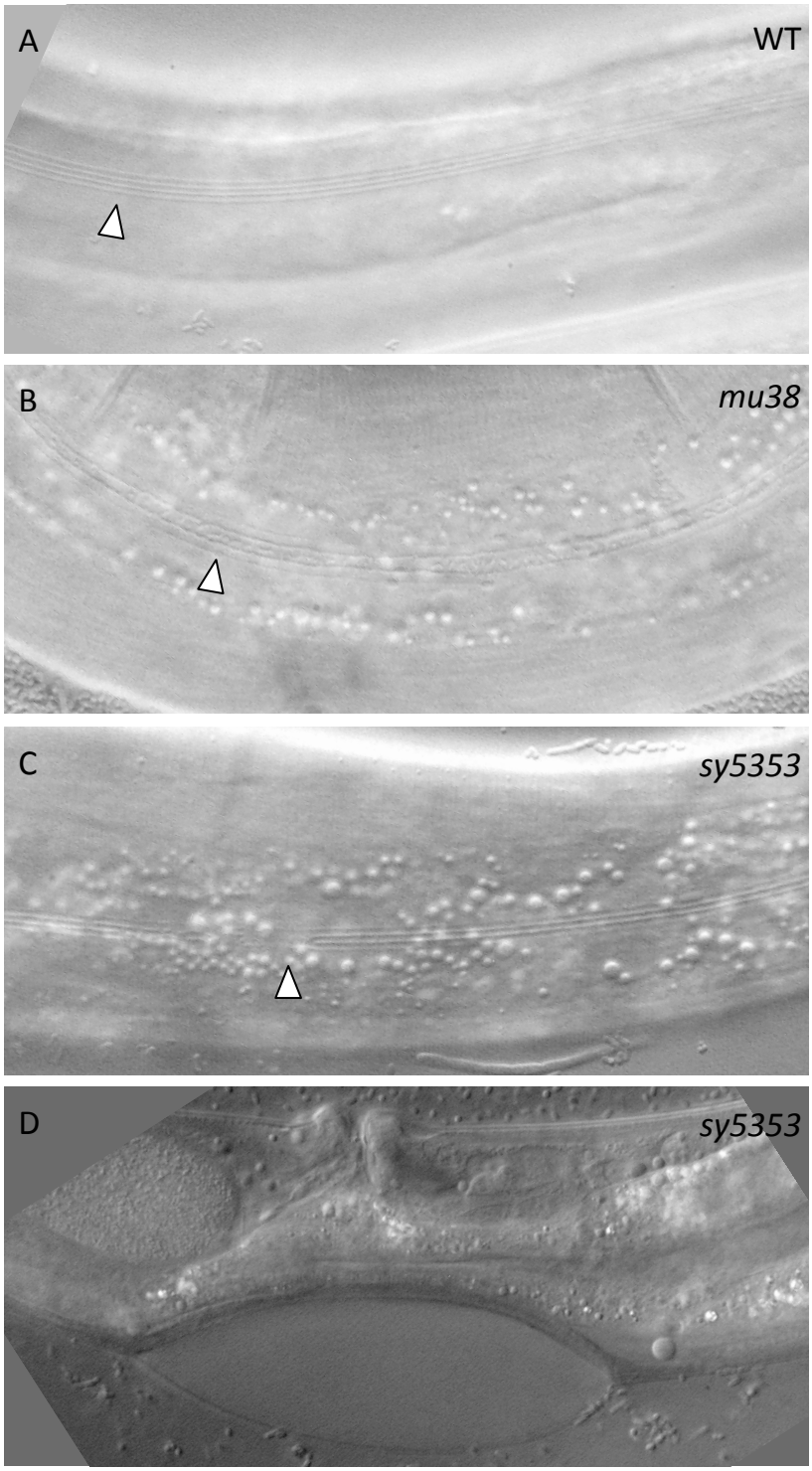

Figure 17. Alae and cuticle defects observed in *pry-1* mutants. Adult *pry-1* mutants exhibit fragmented alae (*mu38,* B), and breaks in the alae (*sy5353,* C) compared to normally continuous alae in the wild type (A). *Cbr-pry-1(sy5353)* also displays blisters in the cuticle (D).

Chapter 5 – Conclusions and Future Directions

Evolutionarily conserved cellular signaling pathways are crucial to the survival of all multicellular organisms, from *Caenorhabditis* to humans. The proper regulation and interactions of these signal transduction pathways orchestrate key cellular events that are indispensible for normal growth and development of these species, and perturbation of the regulation and activity of these pathways can result in a number of pathologies. The study of these conserved pathways, such as the Wnt signaling pathway, allow us to tease apart these pathway interactions, and gain an understanding of the indispensable cellular processes that are affected by aberrant Wnt signaling activity. Using the model organisms *C. elegans* and *C. briggsae* allows for the comparative study of gene regulation in Wnt signaling throughout development in a simple system. However, the study of Wnt signaling in these nematodes has been impeded by the lack of knowledge of the downstream gene targets of the Wnt pathway, and how the expression of these genes is regulated through Wnt signaling pathway activity. The goal of this study was to expand our knowledge of nematode Wnt pathway function and regulation via identification of downstream Wnt pathway target genes. Based on our analysis we have uncovered a novel interaction between the Wnt pathway and the Hedgehog pathway that appears to be conserved between *C. elegans* and *C. briggsae*. Additionally, our results suggest that a key negative regulator of Wnt signaling, *pry-1/Axin,* is itself a genetic target

of the Wnt signaling pathway, acting in an autoregulatory role to control pathway activity.

5.1 *pry-1/Axin* is a putative target of the Wnt signaling pathway

We have undertaken an in-depth analysis of the *pry-1/Axin* gene expression profile in the background of Wnt component knockdowns in both *C. elegans* and *C. briggsae*. Our results suggest that this negative regulator of Wnt signaling activity is itself a target of the Wnt pathway, presumably acting in a negative feedback loop to modulate signaling in these nematode species. Our qRT-PCR and GFP reporter analysis of *pry-1* expression levels in the presence of up- and down-regulated Wnt signaling pathway activity has revealed that *pry-1* expression is responsive to Wnt signaling activity, and this phenomenon is conserved between *C. elegans* and *C. briggsae.* Canonical Wnt signaling has been shown to regulate the expression of many pathway components including Axin2 in vertebrate studies, indicating that feedback control is a conserved feature of Wnt signaling regulation (Jho et al., 2002; Lustig et al.; 2002, Yan et al., 2001). It is interesting to note that this autoregulation of *pry-1/Axin* may have further implications than simply regulation of Wnt pathway activity. Axin is known to play a role as a scaffolding protein mediating multiple cellular signaling pathways, including an interaction with MAP kinase kinase kinases (MEKK) that leads to JNK pathway activation. These interacting pathways control diverse cellular functions ranging from fate specification to tumor suppression, and the

relationship between Wnt pathway control of *pry-1/Axin* and the effect of these interactions should not be disregarded going forward (Luo and Lin, 2003).

We found one intriguing case where the putative conserved autoregulatory role for *pry-1* appears to present differentially between the two nematode species. In *C. briggsae,* RNAi knockdown of *cbr-pop-1* in the wild type background resulted in an increase in *pry-1* expression of over 3 fold compared to the vector control (Figure 8). Conversely, in the wild type *C. elegans* background, a slight reduction in *pry-1* expression was observed in the presence of *pop-1* RNAi knockdown. This seemingly differential role of *pop-1* between these sister species is not the first to have been explored in the nematodes. It was previously discovered that knockdown of POP-1 results in differences in endomesoderm specification in the developing embryo in *C. briggsae* as compared to *C. elegans*. Specifically, loss of POP-1 in *C. elegans* results in the mis-specification of the mesodermal precursor MS to an endoderm (E) type fate in the 8-cell stage blastomere. However, the opposite was found in *C. briggsae,* where RNAi knockdown of *pop-1* results in an E to MS transformation. This was found to be a result of differences in how the *end* gene family of endoderm-specifying genes are regulated by POP-1 in these two species (Lin et al., 2009). The opposing *pop-1* knockdown effect on *pry-1* expression we have observed in *C. elegans* and *C. briggsae* may be indicative of a similar difference in the downstream genes regulated by POP-1 in these two species, either directly or indirectly affecting Wnt

pathway targets and thus *pry-1* expression in the worm.

5.1.1 Future Directions

A key feature of bona fide Wnt pathway transcriptional target genes includes not only changes in gene expression in response to pathway activity, but the presence of TCF/POP-1 transcription factor regulatory elements that are essential for the Wnt effector POP-1 to regulate target gene expression in a Wnt-dependent manner. While we have identified the presence of these sites in the UTR of *pry-1* in both *C. elegans* and *C. briggsae*, a dissection of the essential promoter regions for *pry-1* expression in these two species will clarify its status as a genuine target of the Wnt pathway.

An interesting finding uncovered in this study that is worth pursuing is the role of the second Axin homolog in the nematode species*, axl-1.* Contrary to our result in the *pry-1* mutant background, we observed no increase in *pry-1* expression level in the *C. elegans axl-1* mutant background. In fact, a reduction in *pry-1* expression was observed. This suggests that if *pry-1* is a bona fide target of the Wnt pathway, *axl-1* may not be involved in the negative regulation of this aspect of Wnt signaling control of target gene expression. The differential roles of *pry-1* and *axl-1* have only been preliminarily examined, but it has been suggested that these proteins are not functionally interchangeable, and the function of vertebrate Axin may be divided between these orthologs in negatively regulating canonical BAR-1/β-catenin Wnt signaling during *C. elegans* development

(Oosterveen et al., 2007). A greater understanding of these facets of Wnt pathway regulation will allow for a broader field of view of how the Wnt signaling pathway, and thus expression of its downstream targets, is coordinated in the nematode species. It will also be valuable to examine the degree of conservation in Wnt pathway regulation that exists both between the nematode species, and with other vertebrate species including humans.

5.2 Identification of Wnt pathway target genes in *C. elegans* and *C. briggsae*

The principal mechanism by which the Wnt pathway regulates cellular and developmental processes is through regulation of transcriptional target gene expression. Included among the varied targets of the vertebrate Wnt pathway are genes involved in a multitude of cellular processes, ranging from cell cycle regulators to transcription factors and components of the Wnt pathway itself. Given the highly diverse roles of Wnt signaling that have been characterized in nematode development, a surprisingly small list of genes targeted by the canonical Wnt pathway have been identified thus far in the nematode. In this study we aimed to identify and compare Wnt pathway target genes in *C. elegans* and *C. briggsae* to aid in the analysis of Wnt signaling related processes in this simple model organism, and to further the development of the nematode as a viable model for Wnt signaling pathway studies.

5.2.1 Isolation of genetic suppressors of the *Cbr-pry-1(sy5353)* Muv phenotype

The goal of our forward genetic screen for suppressors of the Muv phenotype in *Cbr-pry-1(sy5353)* was to identify both Wnt target genes and also to isolate mutants in *C. briggsae* Wnt pathway components, as *Cbr-pry-1* is the only Wnt component for which there are mutant strains available. Access to Wnt pathway mutants in *C. briggsae* would make comparative studies of the regulation and function of Wnt signaling in development much simpler. We determined the chromosomal location of two *Cbr-pry-1* Muv phenotype suppressor mutations, one on Chromosome 4 and one on the right arm of Chromosome 1, and the search is on for the identity of these suppressor genes via more precise SNP mapping techniques.

With the growing focus on the establishment of new technologies, the comparative evolutionary approach to the study of developmental signaling pathways including Wnt signaling becomes more attainable. For instance, an alternative approach for mutant gene identification, mapping via whole genome sequencing, has become an increasingly popular method to determine the identity of unknown mutant genes as the PCR-based methods of polymorphism mapping are labour intensive (Hobert, 2010; Minevich et al., 2012). Furthermore, the emerging technologies of genome editing with the CRISPR-Cas9 system which is being developed for use in *C. briggsae* in our lab could be used to generate targeted, heritable alterations in *C. briggsae* gene homologs of *C.*

elegans Wnt pathway components for use in our comparative studies (Friedland et al., 2013).

5.2.2 Comparative transcriptomics uncovers a conserved interaction between the Wnt and Hedgehog signaling pathways in *C. elegans* and *C. briggsae*

For further investigation of Wnt pathway target genes in both *C. elegans* and *C. briggsae,* we have performed a RNA-seq analysis comparing gene expression in the wild type and negative Wnt pathway regulator *pry-1* mutant backgrounds of both species. The results of this analysis have exposed an interaction between the Wnt and Hedgehog signaling pathways, and the processes of molting and cuticle development more generally, which is conserved in both *C. elegans* and *C. briggsae.* This is a novel finding as no direct interactions between the Wnt and the significantly diverged *C. elegans* Hh pathways have been explored in the nematode species as of yet. However, there has been some evidence of crosstalk between the Hh and Wnt pathways in the progression of human gastric cancers, which also demonstrated an inverse correlation between Wnt pathway activation and Hh pathway activation (Yanai et al., 2008).

A previous link between Wnt signaling and cuticle development involves an interesting role of the Wnt pathway in maintaining the seam cell progenitor fate during the larval stem-cell like asymmetric divisions of the epithelial seam cells, which terminally differentiate to form the alae (Gleason and Eisenmann, 2010;

Gorrepati et al., 2013; Ren and Zhang, 2010). Though this process was found to involve the Wnt/ β-catenin asymmetry pathway and not the canonical Wnt pathway, some of the same signaling components are shared between these pathways and this connection will be further examined.

It is interesting to note that the established canonical Wnt pathway target Hox genes *mab-5, lin-39,* and *egl-5* were not uncovered as significantly differentially regulated in our analysis. This is likely due to the isolated increases in Hox gene expression being both temporally regulated and cell-type specific, occurring in a small subset of cells which our methods did not have the sensitivity to resolve.

5.2.3 Future Directions

Validation of our defined set of Hedgehog and molting-related target genes developed based on this RNA-seq analysis has begun in *C. elegans*, but there is much yet to be done to confirm an interaction between the Wnt pathway and these processes. Those putative downstream Wnt target genes that are successfully validated by qRT-PCR will be analyzed for regulatory sequences, spatio-temporal expression patterns, and synergistic phenotypic interactions with Wnt pathway components.

It would firstly be beneficial to determine if the genes we have isolated from our analysis are direct targets of the Wnt pathway. This can be accomplished via identification of essential TCF/POP-1 binding sites in the

regulatory regions of our candidate target genes. Further evidence for a direct target relationship can be provided by examining the control of Wnt pathway activity on expression of these putative gene targets via the completion of a more rigorous qRT-PCR analysis, similar to what we have completed in *pry-1,* for these candidate genes, examining the levels of expression in the background of additional Wnt pathway components such as *bar-1* and *pop-1*.

It is likely the relationship between Wnt signaling and our targets is more complex than a direct target relationship due to the fact that the expression of these candidate genes did not correlate with pathway activity, in fact these genes show reduced expression levels in the *pry-1* mutant background of both species, in which Wnt pathway activity is constitutively active. It may be that the expression of these genes is being modulated by an intermediate direct target of the Wnt pathway that is yet to be identified.

Further analysis can be undertaken to tease apart the Wnt and Hh pathway interactions to determine their relationship. A *C. elegans pry-1* mutant in an RNAi hypersensitive background (*rrf-3*) has been built to investigate RNAi-mediated reduction of target gene function in the background of the *pry-1* mutation to identify any synergistic phenotypic effects suggestive of an interaction. Several phenotypes have been reported in RNAi knock down of Hedgehog pathway genes that can be observed, including defects in molting, growth, alae formation, and endocytosis (Zugasti, 2005). Wnt pathway

component mutants will also be more stringently tested for the presence of these phenotypes. Finally, GFP reporter lines are available for our Hh-r gene targets in *C. elegans.* These can be obtained and the spatial and temporal expression pattern of these genes examined and compared in wild type and Wnt pathway mutant backgrounds such as *pry-1(mu38)* (Hao et al., 2006). This comprehensive and comparative analysis of Wnt signaling interactions with the putative target genes established in this study will allow us to further elucidate the function and regulation of the Wnt pathway in nematode development, and the evolutionary conservation of these features among the nematode species to further the development of the nematode as a viable model for Wnt signaling pathway studies.

References

Blumenthal, T. and Steward, K. (1997). RNA processing and Gene Structure. In Riddle, D. L., Blumenthal, T., Meyer, B.J., and Priess, J.R. (Eds.), *C. elegans II.* (2 ed., Chapter 6). Cold Spring Harbor (NY): Cold Spring Harbor Laboratory Press.

Boulin, T. and Hobert, O. (2012). From genes to function: the *C. elegans* genetic toolbox. WIREs Dev Biol *1,* 114–137.

Brenner, S. (1974). The genetics of *Caenorhabditis elegans.* Genetics *77,* 71-94.

Bürglin, T. R. and Kuwabara, P. E. (2006). Homologs of the Hh signalling network in *C.elegans.* In WormBook, T.c.e.R. Community, ed. (WormBook).

Cartharius, K., Frech, K., Grote, K., Klocke, B., Haltmeier, M., Klingenhoff, A., Frisch,
M., Bayerlein, M., and Werner, T. (2005). MatInspector and beyond: promoter analysis based on transcription factor binding sites. Bioinformatics *21,* 2933-2942.

Chia, I.V. and Costantini, F. (2005). Mouse axin and axin2/conductin proteins are functionally equivalent in vivo. Mol Cell Biol. *25,* 4371-4376.

Clevers, H., and Nusse, R. (2012). Wnt/β-catenin signaling and disease. Cell *149*, 1192-1205.

Consortium, *C.e.S.* (1998). Genome sequence of the nematode *C. elegans*: a platform for investigating biology. Science *282,* 2012-2018.

Coudreuse, D.Y., Roel, G., Betist, M.C., Destree, O., and Korswagen, H.C. (2006). Wnt gradient formation requires retromer function in Wnt-producing cells. Science *312*, 921-924.

Cutter, A.D. (2008). Divergence times *in Caenorhabditis* and *Drosophila* inferred from direct estimates of the neutral mutation rate. Mol Biol Evol *25,* 778-786.

Eisenmann, D.M. (2005). Wnt signaling. In WormBook, T.C.e.R. Community, ed. (WormBook).

Eisenmann, D.M., Maloof, J.N., Simske, J.S., Kenyon, C., and Kim, S.K. (1998). The β- catenin homolog BAR-1 and LET-60 Ras coordinately regulate the Hox gene lin-39 during *Caenorhabditis elegans* vulval development. Development

(Cambridge, England) *125,* 3667-3680.

Felix, M.A. (2007). Cryptic quantitative evolution of the vulva intercellular signaling network in *Caenorhabditis.* Curr Biol *17,* 103-114.

Frand, A.R., Russel, S., and Ruvkun, G. (2005). Functional Genomic Analysis of *C. elegans* Molting. PLoS Biology *3,* e312.

Friedland, A. E., Tzur, Y. B., Esvelt, K. M., Colaiacovo, M. P., and Church, G. M. (2013). Heritable genome editing in *C. elegans* via a CRISPR-Cas9 system. Nature Methods *10,* 741-743.

Gleason, J.E., and Eisenmann, D.M. (2010). Wnt signaling controls the stem cell-like asymmetric division of the epithelial seam cells during *C. elegans* larval development. Developmental Biology *348,* 58-66.

Gleason, J.E., Korswagen, H.C., and Eisenmann, D.M. (2002). Activation of Wnt signaling bypasses the requirement for RTK/Ras signaling during *C. elegans* vulval induction. Genes Dev *16,* 1281-1290.

Gleason, J.E., Szyleyko, E.A., and Eisenmann, D.M. (2006). Multiple redundant Wnt signaling components function in two processes during *C. elegans* vulval development. Developmental biology *298,* 442-457.

Gorrepati, L., Thompson, K.W., and Eisenmann, D.E. (2013). *C. elegans* GATA factors EGL-18 and ELT-6 function downstream of Wnt signaling to maintain the progenitor fate during larval asymmetric divisions of the seam cells. Development *140,* 2093-2102.

Greenwald, I. (2005). LIN-12/Notch signaling in *C. elegans*. In WormBook, T.C.e.R. Community, ed. (Wormbook).

Gupta, B.P., Johnsen R., and Chen, N. (2007). Genomics and biology of the nematode *Caenorhabditis briggsae.* In WormBook, T.C.e.R. Community, ed. (Wormbook).

Hao, L., Johnsen, R., Lauter, G., Baillie, D., and Bürglin, T.R. (2006). Comprehensive analysis of gene expression patterns of hedgehog-related genes. BMC Genomics *7,* 280.

Herman, M.A., Vassilieva, L.L., Horvitz, H.R., Shaw, J.E., Herman, R.K. (1995). The *C. elegans* gene *lin-44*, which controls the polarity of certain asymmetric cell divisions, encodes a Wnt protein and acts cell nonautonomously. Cell *83*, 101–110.

Hillier, L.W., Miller, R.D., Baird, S.E., Chinwalla, A., Fulton, L.A., Koboldt, D.C., and Waterston, R.H. (2007). Comparison of *C. elegans* and *C. briggsae* Genome Sequences Reveals Extensive Conservation of Chromosome Organization and Synteny. PLoS Biol *5,* e167.

Hillier, L.W., Reinke, V., Green, P., Hirst, M., Marra, M.A., and Waterston, R.H. (2009). Massively parallel sequencing of the polyadenylated transcriptome of *C. elegans*. Genome Res *19,* 657-666.

Hobert, O. (2010). The impact of whole genome sequencing on model system genetics: get ready for the ride. Genetics *184,* 317-319.

Hodgkin, J. (2005). Genetic suppression. In WormBook, T.C.e.R. Community, ed. (Wormbook).

Hoogewijs, D., Houthoofd, K., Matthijssens, F., Vandesompele, J., and Vanfleterenm J.R. (2008). Selection and validation of a set of reliable reference genes for quantitative *sod* gene expression analysis in *C. elegans.* BMC Molecular Biology *9.*

Inoue, T., Oz, H.S., Wiland, D., Gharib, S., Deshpande, R., Hill, R.J., Katz, W.S., Sternberg, P.W. (2004). *C. elegans* LIN-18 is a Ryk ortholog and functions in parallel to LIN-17/Frizzled in Wnt signaling. Cell *118*, 795–806.

Jho, E.H., Zhang, T., Domon, C., Joo, C.K., Fruend, J.N., and Constantini, F. (2002). Wnt/beta-catenin/Tcf signaling induced the transcription of Axin2, a negative regulator of the signaling pathway. Mol Cell Biol *22,* 1172-1183.

Kimble, J., and Hirsh, D. (1979). The postembryonic cell lineages of the hermaphrodite and male gonads in *Caenorhabditis elegans*. Developmental biology *70,* 396-417.

Koboldt, D.C., Staisch, J., Thillainathan, B., Haines, K., Baird, S.E., Chamberlin, H.M., Haag, E.S., Miller, R.D., and Gupta, B.P., eds. (2010). A toolkit for rapid gene mapping in the nematode *Caenorhabditis briggsae* (England).

Korswagen, H.C., Coudreuse, D.Y., Betist, M.C., van de Water, S., Zivkovic, D., and Clevers, H.C. (2002). The Axin-like protein PRY-1 is a negative regulator of a canonical Wnt pathway in *C. elegans.* Genes Dev *16,* 1291-1302.

Kramer, J.M., French, R.P., Park, E.C., and Johnson, J.J. (1990). The *Caenorhabditis elegans rol-6* gene, which interacts with the *sqt-1* collagen gene to determine organismal morphology, encodes a collagen. Mol. Cell Biol. *10*,

2081–2089.

Lammi, L., Arte, S., Somer, M., Jarvinen, H., Lahermo, P., Thesleff, I., Pirinen, S., and Nieminen, P. (2004). Mutations in AXIN2 cause familial tooth agenesis and predispose to colorectal cancer. Am J Hum. Genet. *74,* 1043-1050.

Lee, E., Salic, A., Kruger, R., Heinrich, R., and Kirschner, M.W. (2003). The roles of APC and Axin derived from experimental and theoretical analysis of the Wnt pathway. PLoS Biology *1,* E10.

Li, V.S., Ng, S.S., Boersema, P.J., Low, T.Y., Karthaus, W.R., Gerlach, J.P., Mohammed, S., Heck, A.J., Maurice, M.M., Mahmoudi, T., and Clevers, H. (2012). Wnt signaling through inhibition of β-catenin degradation in an intact Axin1 complex. Cell *149,* 1245-1256.

Lin, K.T.-H., Broitman-Maduro, G., Hung, W. W. K., Cervantes, S., and Maduro, M.F. (2009). Knockdown of SKN-1 and the Wnt effector TCF/POP-1 reveals differences in endomesoderm specification in *C. briggsae* as compared with *C. elegans.* Developmental Biology *325,* 296-306.

Lin, R., Thompson, S., and Priess, J.R. (1995). *pop-1* encodes an HMG box protein required for the specification of a mesoderm precursor in early *C. elegans* embryos. Cell *83*, 599–609.

Liu, W., Dong, X., Mai, M., Seelan, R.S., Taniguchi, K., Krishnadath, K.K., Halling, K.C., Cunningham, J.M., Boardman, L.A., Qian, C., Christensen, E., Schmidt, S.S., Roche, P.C., Smith D.I., and Thibodeau, S.N. (2000). Mutations in AXIN2 cause colorectal cancer with defective mismatch repair by activating beta-catenin/TCF signalling. Nat. Genet. *26,* 146–147.

Luo, W., and Lin, S.-C. (2003). Axin: A master scaffold for multiple signaling pathways. Neurosignals *13,* 99-113.

Lustig, B., Jerchow, B., Sachs, M., Weiler, S., Pietsch, T., Karsten, U., van de Wetering, M., Clevers, H., Schlag, P.M., Birchmeier, W., and Behrens, J. (2002). Negative feedback loop of Wnt signaling through upregulation of conductin/axin2 in colorectal and liver tumors. Mol. Cell. Biol. *22,* 1184–1193.

Maduro, M., and Pilgrim, D. (1995). Identification and cloning of unc-119, a gene expressed in the *Caenorhabditis elegans* nervous system. Genetics *141,* 977-988.

Maloof, J.N., Whangbo, J., Harris, J.M., Jongeward, G.D., and Kenyon, C. (1999).

A Wnt signaling pathway controls hox gene expression and neuroblast migration in *C. elegans.* Development *126,* 37-49.

Mello, C.C., Kramer, J.M., Stinchcomb, D., and Ambros, V. (1991). Efficient gene transfer in *C.elegans*: extrachromosomal maintenance and integration of transforming sequences. EMBO J *10,* 3959-3970.

Minevich, G., Park, D. S., Blackenberg, D., Poole, R. J., and Hobert, O. (2012). CloudMap: A cloud-based pipeline for analysis of mutant genome sequences. Genetics *192,* 1249-1269.

Miskowski, J., Li, Y., and Kimble, J. (2001). The sys-1 gene and sexual dimorphism during gonadogenesis in *Caenorhabditis elegans.* Developmental biology *230,* 61-73.

Oosterveen, T., Coudreuse, D.Y., Yang, P.T., Fraser, E., Bergsma, J., Dale, T.C., and Korswagen, H.C. (2007). Two functionally distinct Axin-like proteins regulate canonical Wnt signaling in *C. elegans.* Developmental Biology *308,* 438-448.

Pénigault, J.B. and Félix, M.A. (2011). High sensitivity of *C. elegans* vulval precursor cells to the dose of posterior Wnts. Developmental Biology *357,* 428-438.

Portman, D.S. (2005). Profiling *C. elegans* gene expression with DNA microarrays. In WormBook, T.C.e.R. Community, ed. (WormBook).

Ren, H., and Zhang, H. (2010). Wnt signaling controls temporal identities of seam cells in *Caenorhabditis elegans.* Developmental Biology *345,* 144-155

Ruvkun, G., and Hobert, O. (1998). The taxonomy of developmental control in *Caenorhabditis elegans.* Science *282,* 2033-2041.

Sawa, H. and Korswagen, H.C. (2013). Wnt signaling in *C. elegans*. In WormBook, T.C.e.R. Community, ed. (Wormbook).

Seetharaman, A., Cumbo, P., Bojanala, N., and Gupta, B. (2010). Conserved mechanism of Wnt signaling function in the specification of vulval precursor fates in *C.elegans* and *C. briggsae.* Developmental biology *346,* 128-139.

Sharanya, D., Thillainathan, B., Marri, S., Bojanala, N., Taylor, J., Filbotte, S., Moerman, D.G., Waterston R.H. and Gupta, B.P. (2012). Genetic control of vulval development in *Caenorhabditis briggsae*. G3 *2,* 1625-1641.

Shioi, G., Shoji, M., Nakamura, M., Ishihara, T., Katsura, I., Fujisawa, H., and

Takagi, S. (2001). Mutations affecting nerve attachment of *Caenorhabditis elegans.* Genetics *157,* 1611-1622.

Sternberg, P.W. (2005). Vulval development. In WormBook, T.C.e.R. Community, ed. (WormBook).

Sulston, J.E., and Horvitz, H.R. (1977). Post-embryonic cell lineages of the nematode, *Caenorhabditis elegans.* Developmental biology *56,* 110-156.

Sulston, J.E., and White, J.G. (1980). Regulation and cell autonomy during postembryonic development of Caenorhabditis elegans. Developmental biology *78,* 577- 597.

Sulston, J.E., Schierenberg, E., White, J.G., and Thomson, J.N. (1983). The embryonic cell lineage of the nematode Caenorhabditis elegans. Developmental biology *100,* 64-119.

Stein, L.D., Bao, Z., Blasiar, D., Blumenthal, T., Brent, M.R., Chen, N., Chinwalla, A., Clarke, L., Clee, C., Coghlan, A., *et al.* (2003). The genome sequence of *Caenorhabditis briggsae:* a platform for comparative genomics. PLoS Biol *1,* E45.

Wang, Z., Gerstein, M., and Snyder, M. (2009) RNA-seq: a revolutionary tool for transcriptomics. Nature Reviews Genetics *10,* 57-63.

Whangbo, J., Kenyon, C. (1999). A Wnt signaling system that specifies two patterns of cell migration in *C. elegans*. Mol. Cell *4*, 851–858.

Winston, W.M., Sutherlin, M., Wright, A.J., Feinberg, E.H., and Hunter, C.P. (2007). *Caenorhabditis elegans* SID-2 is required for environmental RNA interference. Proc Natl Acad Sci USA *104,* 10565-10570.

Yan, D., Wiesmann, M., Rohan, M., Chan, V., Jefferson, A.B., Guo, L., Sakamoto, D., Caothien, R.H., Fuller, J.H., Reinhard, C., Garcia, P.D., Randazzo, F.M., Escobedo, J., Fantl, W.J., and Williams, L.T. (2001). Elevated expression of axin2 and hnkd mRNA provides evidence that Wnt/beta-catenin signaling is activated in human colon tumors. Proc Natl Acad Sci USA *98,* 14973-14978.

Yanai, K., Nakamura, M., Akiyoshi, T., Nagai, S., Wada, J., Koga, K., Noshiro, H., Nagai, E., Tsuneyoshi, M., Tanaka, M., and Katano, M. (2008). Crosstalk of hedgehog and Wnt pathway in gastric cancer. Cancer Letters *263,* 145-156.

Zhao, Z., Flibotte, S., Murray, J.I., Blick, D., Boyle, T.J., Gupta, B., Moerman, D.G., and Waterston, R.H., eds. (2010). New tools for investigating the

comparative biology of *Caenorhabditis briggsae* and *C. elegans.* Genetics *184,* 853-863.

Zinovyeva, A.Y., Yamamoto, Y., Sawa, H., and Forrester, W.C. (2008). Complex network of Wnt signaling regulates neuronal migrations during *Caenorhabditis elegans* development. Genetics *179*, 1357-1371.

Zugasti, O., Rajan, J., and Kuwabara, P.E. (2005). The function and expansion of the Patched- and Hedgehog-related homologs in *C. elegans.* Genome Research *15,* 1402- 1410.